JCI insight

Chemotherapy followed by anti-CD137 mAb immunotherapy improves disease control in a mouse myeloma model

Camille Guillerey, Kyohei Nakamura, Andrea C. Pichler, Deborah Barkauskas, Sophie Krumeich, Kimberley Stannard, Kim Miles, Heidi Harjunpää, Yuan Yu, Mika Casey, Alina I. Doban, Mircea Lazar, Gunter Hartel, David Smith, Slavica Vuckovic, Michele W.L. Teng, P. Leif Bergsagel, Marta Chesi, Geoffrey R. Hill, Ludovic Martinet, Mark J. Smyth

JCI Insight. 2019. https://doi.org/10.1172/jci.insight.125932.

Research In-Press Preview **Immunology**

Immunotherapy holds promise for multiple myeloma (MM) patients but little is known about how MM-induced immunosuppression influences response to therapy. Here, we investigated the impact of disease progression on immunotherapy efficacy in the Vk*MYC mouse model. Treatment with agonistic anti-CD137 (4-1BB) mAbs efficiently protected mice when administered early but failed to contain MM growth when delayed more than three weeks after Vk*MYC tumor cell challenge. The quality of $CD8^+$ T cell response to CD137 stimulation was not altered by the presence of MM, but $CD8^+$ T cell numbers were profoundly reduced at the time of treatment. Our data suggest that an insufficient ratio of $CD8^+$ T cells over MM cells (CD8/MM) accounts for the loss of anti-CD137 mAb efficacy. We established serum M-protein levels prior to therapy as a predictive factor of response. Moreover, we developed an *in silico* model to capture the dynamic interactions between $CD8^+$ T cells and MM cells. Finally, we explored two methods to improve the CD8/MM ratio: anti-CD137 mAb immunotherapy combined with Treg-depletion or administered after chemotherapy treatment with cyclophosphamide or melphalan efficiently reduced MM burden and prolonged survival. Altogether, our data indicate that consolidation treatment with anti-CD137 mAbs might prevent MM relapse.

Chemotherapy followed by anti-CD137 mAb immunotherapy improves disease control in a mouse myeloma model.

Camille Guillerey[1,2,3], Kyohei Nakamura[1], Andrea C. Pichler[4], Deborah Barkauskas[1], Sophie Krumeich[1], Kimberley Stannard[1], Kim Miles[1], Heidi Harjunpää[2,5], Yuan Yu[1], Mika Casey[1], Alina I. Doban[6], Mircea Lazar[7], Gunter Hartel[8], David Smith[8], Slavica Vuckovic[9,10], Michele W.L. Teng[5], P. Leif Bergsagel[11], Marta Chesi[11], Geoffrey R. Hill[9,12], Ludovic Martinet[4], Mark J. Smyth[1,2].

[1]Immunology in Cancer and Infection Laboratory, QIMR Berghofer Medical Research Institute, Herston, Queensland, Australia; [2]School of Medicine, The University of Queensland, Herston, Queensland, Australia; [3]New address: Cancer Immunotherapies Laboratory, Mater Research Institute, The University of Queensland, Translational Research Institute, Woolloongabba, Brisbane, QLD, Australia. [4]Cancer Research Center of Toulouse, INSERM UMR 1037, Toulouse, France.[5]Cancer Immunoregulation and Immunotherapy Laboratory, QIMR Berghofer Medical Research Institute, Herston, Queensland, Australia; [6]ASML Netherlands B.V., Veldhoven, The Netherlands; [7]Department of Electrical Engineering, Eindhoven University of Technology, P.O. Box 513, Eindhoven 5600 MB, The Netherlands; [8]Statistics Unit, QIMR Berghofer Medical Research Institute, Herston, Queensland, Australia; [9]Bone Marrow Transplantation Laboratory, QIMR Berghofer Medical Research Institute, Herston, Queensland, Australia; [10]Multiple Myeloma Research Group, Institute of Haematology, Royal Prince Alfred Hospital, NSW, 2050, Australia; [11]Comprehensive Cancer Center, Mayo Clinic, Scottsdale, AZ, USA; [12]Fred Hutchinson Cancer Research Center 1100 Fairview Ave N, Seattle, WA98109, USA;

Corresponding author: Dr Camille Guillerey, QIMR Berghofer Medical Research Institute, 300 Herston Road, Herston, 4006, Australia. New address: Cancer Immunotherapies Laboratory, Mater Research Institute, The University of Queensland, Translational Research Institute, Woolloongabba, Brisbane, QLD, Australia. E-mail address: camille.guillerey@mater.uq.edu.au, Phone: +61-7-3443-7519.

Conflict of interest statement: M. J. Smyth has research agreements with Bristol Myers Squibb, Tizona Therapeutics, and Aduro Biotech. All the other authors declare that they have no conflict of interest.

Abstract: Immunotherapy holds promise for multiple myeloma (MM) patients but little is known about how MM-induced immunosuppression influences response to therapy. Here, we investigated the impact of disease progression on immunotherapy efficacy in the Vk*MYC mouse model. Treatment with agonistic anti-CD137 (4-1BB) mAbs efficiently protected mice when administered early but failed to contain MM growth when delayed more than three weeks after Vk*MYC tumor cell challenge. The quality of $CD8^+$ T cell response to CD137 stimulation was not altered by the presence of MM, but $CD8^+$ T cell numbers were profoundly reduced at the time of treatment. Our data suggest that an insufficient ratio of $CD8^+$ T cells over MM cells (CD8/MM) accounts for the loss of anti-CD137 mAb efficacy. We established serum M-protein levels prior to therapy as a predictive factor of response. Moreover, we developed an *in silico* model to capture the dynamic interactions between $CD8^+$ T cells and MM cells. Finally, we explored two methods to improve the CD8/MM ratio: anti-CD137 mAb immunotherapy combined with Treg-depletion or administered after chemotherapy treatment with cyclophosphamide or melphalan efficiently reduced MM burden and prolonged survival. Altogether, our data indicate that consolidation treatment with anti-CD137 mAbs might prevent MM relapse.

Introduction

Multiple myeloma (MM) is a hematological malignancy where clonal plasma cells secreting monoclonal proteins (M-proteins) proliferate in the bone marrow (BM). Standard treatment options include autologous stem cell transplantation for eligible patients, as well as alkylating agents such as cyclophosphamide, proteasome inhibitors such as bortezomib and immunomodulatory drugs (IMiDs) (1). Despite high response rates to standard therapies, most MM patients relapse and eventually succumb to the disease. Therefore, new therapeutic options with different mechanisms of action are urgently needed to eradicate residual disease and achieve long-term remission.

A variety of immune-based therapies are now being explored, with the potential to overcome MM cell resistance to conventional drugs (2). Elotozumab (anti-SLAMF7) and daratumumab (anti-CD38) are two monoclonal antibodies (mAbs) that were FDA approved in 2015 for the treatment of relapsed/refractory MM patients (3). These mAbs target molecules expressed on MM cells and exert their anti-tumor effect through multiple mechanisms including immune-modulation. Many other immune-based strategies are currently in development, such as bispecific antibodies, infusions of ex vivo expanded/activated autologous T or NK cells, TCR-modified T cells and chimeric antigen-receptor T and NK cells (4). Immune checkpoint inhibition is also considered for the treatment of MM. A phase I clinical study reported disease stabilization, but no objective response, in relapsed/refractory MM patients treated with single agent anti-PD-1 blocking mAb nivolumab (5). Moreover, in spite of encouraging response rates, a phase II clinical study examining the anti-PD-1 mAb pembrolizumab in combination with IMiDs had to be terminated due to increased risk of severe adverse events (6).

Agonistic mAbs targeting costimulatory molecules represent an alternative to checkpoint inhibitors (7). CD137 (4-1BB) is a co-stimulatory molecule expressed on activated T cells and NK cells as well as antigen presenting cells and endothelial cells (8). Upon ligation, CD137 signals through nuclear factor (NF)-κB and the MAPK cascade to promote cell survival, proliferation and enhanced effector functions (9). Recent evidence indicates that CD137 costimulation augments the mitochondrial mass of $CD8^+$ T cells (10). CD137 costimulation also induces chromatin remodeling and thereby imprints long-term changes in $CD8^+$ T cells (11).

Agonistic anti-CD137 mAbs promote Th1 type responses and have shown activity in a number of mouse syngeneic tumor models, including mouse models of MM and plasmacytomas (12, 13). The anti-tumor effect of anti-CD137 mAbs in mice generally depends on IFNγ and $CD8^+$ T cells while $CD4^+$ T cells and NK cells are either required or dispensable depending on the tumor model (14). Notably, in the Vk*MYC model of mouse MM, anti-CD137 mAb immunotherapy was found to require $CD8^+$ T cells and NK cells but not $CD4^+$ T cells (12). Furthermore, recent work highlighted the essential role BATF3-dependent dendritic cells (DCs) in cross-priming $CD8^+$ T cells specific to tumor antigens and their importance for the response to anti-CD137 mAb therapy (15).

Two fully humanized anti-CD137 mAbs have entered clinical trials: Urelumab (BMS-663513) and Utomilumab (PF-05082566). Doses of acceptable toxicities had to be defined for Urelumab since this mAb had caused severe liver damage at high doses (16). By contrast, only mild toxicities were observed with Utomilumab (17, 18). In phase I/II clinical trials, both mAbs have shown signs of immunologic activity associated with an IFN-response (16, 17). Therefore, anti-CD137 mAbs hold promise for the treatment of a broad range of malignancies, including MM where Urelumab is now being assessed in combination with Elotuzumab (NCT02252263).

Since host-related immunodeficiency is frequently observed in MM (19, 20), a better understanding of how MM-induced immunosuppression impacts on immunotherapy efficacy is needed to define the best therapeutic conditions and to identify prognostic markers. In this study, we investigated the factors determining the efficacy of agonistic anti-CD137 mAb immunotherapy in the Vk*MYC model of mouse MM. We combined *in vivo, ex vivo* and *in silico* analyses to investigate the dynamic interactions between $CD8^+$ T cells and MM cells in the BM of anti-CD137 mAb-treated mice. Overall, our data indicate that single agent anti-CD137 mAb therapy is only efficient against low MM burden. Yet, we show that at advanced disease stages, therapeutic efficacy of anti-CD137 mAb can be achieved by releasing immunosuppression through Treg-depletion or by “debulking” the tumor through chemotherapy.

Results

Early anti-CD137 mAb treatment induces potent effector T cell responses and protects mice against MM with negligible toxicity.

To evaluate the efficacy of anti-CD137 mAbs against MM, we challenged C57BL/6 WT mice with Vk12653 (Vk*MYC) MM cells followed by 2-week treatment with anti-CD137 mAbs starting from 2 weeks after tumor inoculation. Anti-CD137 mAb treatment significantly prolonged the survival of MM-challenged mice, with 68% (13/20) of the anti-CD137 mAb-treated mice becoming long-term survivors (Figure 1A). Moreover, monoclonal gammopathy at week 5 post Vk*MYC cell-injection was clearly reduced in anti-CD137 mAb-treated mice (Figure 1B). Mice treated with anti-CD137 mAbs harbored significantly reduced numbers of MM cells (Figure 1C), and increased numbers of $CD8^+$ T cells and $FoxP3^-CD4^+$ T helper cells in the BM and spleen (Figures 1D and E). These data confirm our previous findings that anti-CD137 mAbs induce massive T cell expansion and provide long-term protection against MM (12).

To gain further insight into the quality of the T cell response induced following anti-CD137 mAb treatment, cytokine production was analyzed by intracellular staining. We found that anti-CD137 mAb treatment increased the percentage of IFNγ- and TNF-producing $CD4^+$ and $CD8^+$ T cells in the BM and spleen (Figures 2A and B). We also observed an increase in IL10-producing T cells, with BM $CD4^+$ T cells being the most important IL10 producers. Moreover, we analyzed the memory status of BM $CD8^+$ T cells and observed a large increase in $CD44^+CD62L^-$ effector/effector-memory cells (TEM) following anti-CD137 mAb injection into both tumor-naïve and MM-bearing mice (Figure 2C and Supplemental Figure 1).

Since the potent T cell responses induced by anti-CD137 mAbs may lead to tissue damage, and notably hepatotoxicity (21), we measured serum levels of the liver enzymes alanine transaminase (ALT) and aspartate transaminase (AST) as well as T cell and tumor cell infiltration of the liver. AST levels were significantly increased in control IgG- but not anti-CD137 mAb-treated mice (Supplemental Figure 2A), probably reflecting liver damage caused by the tumor (Supplemental Figure 2B). The livers of anti-CD137 mAb-treated mice harbored very low numbers of MM cells but showed increased lymphocytic infiltrates, including $CD8^+$ T cells and $FoxP3^+$ Tregs (Supplemental Figure 2, B-F). Overall, anti-CD137

mAb treated mice appeared healthy and we did not observe obvious external signs of autoimmunity nor inflammation. Taken together, these data indicate that anti-CD137 mAbs induce strong effector T cell responses that efficiently protect mice against MM with negligible liver damage.

CD137 stimulation induces transient NK cell responses followed by T cell proliferation and IFNγ production.

We previously reported that, in the Vk*MYC MM model, therapeutic efficacy of anti-CD137 mAbs requires the presence of both NK cells and $CD8^+$ T cells (12). To gain further insight into the kinetics of lymphocyte responses to CD137 stimulation, tumor-naïve WT mice were given a single injection of anti-CD137 mAbs on day 0, and NK cell and T cell proliferation and IFNγ production were analyzed in the BM and spleen on day 1, 3 and 7. By day 3 post anti-CD137 mAb injection, NK cell responses had reached their maximum and we observed a significant increase in the percentages of proliferating and IFNγ-producing NK cells when compared with IgG-treated mice (Figure 3, A-D and Supplemental Figure 3, A-B). By contrast, on day 3, percentages of proliferative $CD4^+$ and $CD8^+$ T cells were only slightly increased in anti-CD137 mAb treated mice and there was virtually no change in IFNγ production compared to control IgG treated mice. However, on day 7, we observed strong T cell proliferation and IFNγ production in mice that had received anti-CD137 mAbs. We also measured systemic levels of IFNγ and observed a slight increase on day 7 post-CD137 mAb injection (Supplemental Figure 3C). Of note, the magnitude of T cell responses was higher in the BM (Figure 3, A-D) than in the spleen (Supplemental Figure 3, A-B). In agreement with previous reports (22-24), we observed reduced numbers and percentages of NK cells in mice injected with anti-CD137 mAbs (Figure 3, E-F). This decrease was more striking in the spleen than in the BM. We obtained similar results when NK cells were gated either as $TCR\beta^-$ $NK1.1^+$ or $TCR\beta^-$ $NKp46^+$ cells (data not shown). Altogether, these data indicate that NK cells are the first lymphocytes to respond to CD137 stimulation, but NK cell responses are transient. By day 7 post anti-CD137 mAb injection, the majority of NK cells had disappeared while T cells showed robust proliferation and IFNγ production.

IFNγ signaling is required for CD8$^+$ T cell expansion and optimal efficacy of anti-CD137 mAb therapy.

To investigate the importance of IFN-signaling for CD8$^+$ T responses to CD137 stimulation, tumor-naïve WT, *Ifnγ*$^{-/-}$ or *Ifnγr*$^{-/-}$ mice received a 2-week anti-CD137 mAb-treatment. We observed a large increase in CD8$^+$ T cell numbers in the BM and spleen of anti-CD137 mAb-treated WT mice whereas CD8$^+$ T cell expansion in response to anti-CD137 mAb treatment was compromised in the spleen of *Ifnγ*$^{-/-}$ mice and in the BM and spleen of *Ifnγr*$^{-/-}$ mice (Figure 4A and Supplemental Figure 4A). Yet, percentages of CD44$^+$CD62L$^-$ TEM CD8$^+$ T cell were increased in *Ifnγr*$^{-/-}$ mice following anti-CD137 mAb treatment (Supplemental Figure 4B), indicating that, in spite of their limited expansion, CD8$^+$ T cells do respond to CD137 stimulation in the absence of IFNγ-signaling. By contrast, anti-CD137 mAb-treatment increased the numbers of BM CD8$^+$ T in *Ifnar*$^{-/-}$ mice, indicating that type I IFNs are not essential for CD8$^+$ T expansion following CD137 stimulation (Supplemental Figure 4C).

Next, we analyzed the IFN-requirement of anti-CD137 mAbs for their anti-MM effect. We observed that the efficacy of anti-CD137 mAbs against MM was compromised in *Ifnγ*$^{-/-}$ mice (Figure 4B). Interestingly, lack of treatment efficacy was associated with decreased CD8$^+$ T cell numbers in the BM of anti-CD137 mAb treated *Ifnγ*$^{-/-}$ mice compared to WT mice (Figure 4C) as well as increased IL10 production by CD4$^+$ T cells (Figure 4, D-E). Of note, anti-CD137 mAb treatment could not be tested in *Ifnγr*$^{-/-}$ mice because these mice failed to develop MM when challenged with Vk*MYC MM cells (data not shown), probably because of high circulating levels of IFNγ (Supplemental Figure 4D). In agreement with their ability to expand CD8$^+$ T cells in the absence of type I IFN signaling, anti-CD137 mAbs efficiently protected *Ifnar*$^{-/-}$ mice against MM (Supplemental Figure 4E). All together, these data demonstrate that IFNγ contributes to CD8$^+$ T cell expansion and is essential for efficient anti-CD137 mAb therapy in the Vk*MYC mouse model of MM.

Anti-CD137 mAb-treatment loses efficacy when delayed more than 3 weeks after Vk*MYC cell-challenge.

So far, our data have established that anti-CD137 mAb-treatment efficiently protects against MM when given at week 2 post-Vk*MYC cell challenge. At this time point, a very low percentage of MM cells (<1%) is detectable in the BM and the tumor has not yet spread to the spleen (Supplemental Figures 5A and

B). To determine whether anti-CD137 mAb treatment could be delayed to treat advanced disease stages, MM-challenged WT mice were given a 2-week anti-CD137 mAb treatment starting from week 1, 2, 3 or 4 after Vk*MYC cell injection (Supplemental Figure 5C). Tumor burden and serum M-protein level analyses indicated that anti-CD137 mAb treatment lost efficacy when delayed more than 3 weeks after Vk*MYC cell injection (Figures 5A and B).

We hypothesized that MM-induced immunosuppression might contribute to the loss of anti-CD137 mAb efficacy. To gain more insight into the course of natural immune responses to MM, we analyzed IFNγ production by NK cells and T cells in the BM of MM-bearing mice. Interestingly, in mice with low-tumor burden (< 4.8 x 10^5 MM cells), we observed a positive correlation between percentages of IFNγ-producing $CD8^+$ T cells and tumor burden in the BM whereas this correlation became negative in mice with higher tumor burden (> 4.8 x 10^5 MM cells; Figure 5C). By contrast, no correlation was found between the percentages of IFNγ-producing NK cells or $CD4^+$ T cells and tumor burden in the BM (Supplemental Figure 5D). These data indicate that the developing tumor may trigger an initial $CD8^+$ T cell response but this response is then suppressed as the tumor grows. Moreover, percentages of $CD4^+$ and $CD8^+$ T cells producing the immunosuppressive cytokine IL10 positively correlated with tumor burden in the BM (Figure 5D), thereby supporting the idea of progressive immunosuppression. These data suggest that the establishment of a suppressive microenvironment might contribute to the loss of efficacy of anti-CD137 mAbs against MM.

High MM burden does not prevent T cells from responding to CD137 stimulation

To determine whether MM-induced immunosuppression hampers immune cell ability to respond to CD137 stimulation, we analyzed NK cell and T cell responses to a single injection of anti-CD137 mAbs given either at week 2 or at week 4 post Vk*MYC cell challenge. These 2 time points were chosen because very good therapeutic efficacy of anti-CD137 mAbs was obtained at week 2 and protection was lost at week 4 (Figures 5A and B). Intriguingly, while NK cell numbers significantly dropped in response to week-2-anti-CD137 mAb injection, this decrease was much less pronounced at week 4 post Vk*MYC cell challenge (Supplemental Figures 6A and B). Importantly, anti-CD137 mAbs induced T cell proliferation and IFNγ production when given either at week 2 or week 4 post Vk*MYC cell challenge (Figures 6A and B and Supplemental Figures 6C and D). Moreover, there was no correlation

between percentages of IFNγ–producing $CD4^+$ or $CD8^+$ T cells and tumor burden in mice that had received a 2-week-anti-CD137 mAb treatment (Supplemental Figure 6E). Still, we observed a positive correlation between tumor burden and percentages of IL10–producing $CD4^+$ but not $CD8^+$ T cells in these mice (Supplemental Figure 6F). Of note, most of IL10-producing $CD4^+$ T cells were also positive for IFNγ (Supplemental Figures 6G and H). Altogether, these data indicate that T cell exhaustion is unlikely to be the reason for the lack of treatment efficacy; in high-tumor burden bearing mice, $CD4^+$ and $CD8^+$ T cells are still able to respond to CD137 stimulation by proliferating vigorously and by producing IFNγ.

Reduced numbers of $CD8^+$ T cells in association with high-tumor burden might contribute to the lack of efficacy of delayed anti-CD137 mAb treatment.

Even though equivalent $CD8^+$ T cell proliferation was observed in response to week 2 or week 4 anti-CD137 mAb injection, we noticed that the numbers of BM $CD8^+$ T cells obtained post-CD137 stimulation were lower when this injection was given at week 4 (Figure 6C). In the BM of untreated mice, $CD8^+$ T cell numbers dropped drastically when the tumor-burden reached 10^6 malignant plasma cells per femur (Figure 6D). Thus, in mice with high tumor burden, low numbers of BM $CD8^+$ T cells prior to anti-CD137 mAb therapy will result in low numbers of $CD8^+$ T cells post-therapy, in spite of CD137-induced $CD8^+$ T cell proliferation. Of note, the fold increase in $CD8^+$ T cell numbers induced by CD137 stimulation at week 2 was higher than the one at week 4 (increased 4.2 and 1.5 times, respectively), indicating that increased $CD8^+$ T cell death might occur at week 4. Furthermore, the ratio of $CD8^+$ T cells over MM cells (CD8/MM) decreases with time post MM-injection: before week 3 post-MM injection, most of the mice had a CD8/MM ratio above 1 whereas after week 4 this ratio dropped below 1 (Figure 6E). These data support the idea that insufficient CD8/MM ratio contributes to the lack of efficacy of delayed anti-CD137 mAb treatment.

Serum M-protein levels before treatment predict the efficacy of anti-CD137 mAbs

We hypothesized that tumor burden prior to treatment may be a predictive factor of anti-CD137 mAb treatment efficacy. To test this hypothesis, we divided mice into responders and non-responders (Supplemental Figure 7A) and performed a logistic regression of response versus pre-treatment M-protein levels (Figure 7A and Supplemental Figure 7B). This logistic model correctly classified 15/17

(88%) responders as responders and 8/10 (80%) non-responders as non-responders. This model indicates that mice displaying pre-treatment M-protein levels below 7.3% are likely to respond to anti-CD137 mAb treatment (predicted efficacy of 95%) whereas treatment would fail in mice with initial M-proteins levels above 29.4% (predicted failure rate of 95%). Moreover, a partition tree performed on the same data set and using a cut-off value of 10.2% for pre-treatment M-protein levels correctly identified 15 of 17 responders and all 10 non-responders (Figure 7B). Overall these analyses indicate that treatment efficacy depends on initial tumor burden.

***In silico* modeling of CD8$^+$ T cell-MM cell interactions and their impact on treatment efficacy**

To further understand the interactions between CD8$^+$ T cells and MM cells in the BM, we developed a mathematical model by adapting the model recently proposed by Doban et al. (25) to fit our data (see Supplemental methods). This new model utilizes delay differential equations to describe the interactions between 4 populations: MM cells (M), naïve CD8$^+$ T cells (Z), activated CD8$^+$ T cells (A) and exhausted CD8$^+$ T cells (E) (Supplemental Figure 8A). The 4 equations that determine these interactions are shown in Supplemental Methods and are described as follows:

1. Rate of change of MM cell population = MM cell growth – MM cell killing by activated CD8$^+$ T cells
2. Rate of change of activated CD8$^+$ T cell population = proliferation of activated CD8$^+$ T cells + steady state conversion of naïve CD8$^+$ T cells into activated CD8$^+$ T cells + MM-induced conversion of naïve CD8$^+$ T cells into activated CD8$^+$ T (*) + anti-CD137 mAb treatment-induced conversion of naïve CD8$^+$ T cells into activated CD8$^+$ T – contraction of activated CD8$^+$ T cells – MM-induced conversion of activated CD8$^+$ T cells into exhausted CD8$^+$ T cells
3. Rate of change of naive CD8$^+$ T cell population = proliferation/arrival of naive CD8$^+$ T cells – steady state conversion of naïve CD8$^+$ T cells into activated CD8$^+$ T cells – MM-induced conversion of naïve CD8$^+$ T cells into activated CD8$^+$ T (*) – anti-CD137 mAb treatment-induced conversion of naïve CD8$^+$ T cells into activated CD8$^+$ T – suppression of naive CD8$^+$ T cell by MM cells
4. Rate change of exhausted CD8$^+$ T cell population = MM-induced conversion of activated CD8$^+$ T cells into exhausted CD8$^+$ T cells – death of exhausted CD8$^+$ T cells

(*) when the tumor burden is decreasing, there is no MM-induced conversion of naïve $CD8^+$ T cells into activated $CD8^+$ T cells and thus this term is set to zero.

Interactions between these populations are regulated by different parameters such as MM and $CD8^+$ T cell growth rates, conversion rates of naïve into activated $CD8^+$ T cells and of activated into exhausted $CD8^+$ T cells, killing capacity of activated $CD8^+$ T cells and MM suppressive effect (see Supplemental methods). We first selected parameters so that the 4 population dynamics reflected the data we obtained in untreated mice. In these settings, MM tumor grew very slowly until day 21 and then increased rapidly to reach a plateau around day 60 (Figure 8A). In parallel, numbers of naïve $CD8^+$ T cells decreased due to their conversion into activated $CD8^+$ T cells and the suppressive effect of the tumor. The activated $CD8^+$ T cell population increased up to day 12 but as MM grew, these cells were suppressed and converted into exhausted $CD8^+$ T cells that finally died, leading to a profound decrease in total $CD8^+$ T cell numbers. We then defined the best fitting parameters for anti-CD137 mAb treatment under the assumption that this therapy will induce further conversion of naïve $CD8^+$ T cells into activated $CD8^+$ T cells and increase the growth, survival and killing capacity of activated $CD8^+$ T cells (see Supplemental methods and Supplemental Figure 8B). With these parameters, anti-CD137 mAb treatment failed to eradicate the tumor if given at day 25 or later (Figures 8B and C), when the CD8/MM ratio was 0.75. These values are consistent with our measured data in the Vk*MYC MM model (Figures 5A-B and Figure 6E). Interestingly, in these conditions, the ratio of activated $CD8^+$ T cells over MM cells at day 25 was 0.13, indicating that more than 1 effector cell is needed to kill 10 MM cells. We then modified the number of tumor cells reaching the BM or their growth rate to mimic differences between batches of Vk*MYC cells (Table 1). As expected, if more tumor cells reached the BM or if their growth rate was increased, anti-CD137 mAb treatment lost efficacy earlier. Loss of efficacy was also observed earlier when the suppressive effect of MM on activated $CD8^+$ T cells was increased. By contrast, MM suppressive effect on naïve $CD8^+$ T cells only modestly modulated treatment efficacy. Finally, we tested different killing capacities of $CD8^+$ T cells. When anti-CD137 mAb treatment had no effect on activated CD8 T cell killing capacity (i.e. it only induced the conversion of naïve into activated $CD8^+$T cells, increased the growth and survival of activated $CD8^+$ T cells and thus resulted in increased numbers of activated $CD8^+$ T cells without enhanced killing capacity), this 2-week treatment failed to eradicate the tumor when given beyond day 8. Moreover, for the treatment to be efficient beyond 4 weeks post-myeloma injection, the killing capacity of CD8 T cells had to be 10 times higher than the value set up in

untreated conditions. Overall this model captures the complexity of the interactions between $CD8^+$ T cells and MM cells and indicates that anti-CD137 mAb treatment efficacy is dependent on multiple parameters, including CD8/MM ratio, MM growth rate, MM suppressive activity and treatment ability to stimulate efficient $CD8^+$ T cell-mediated killing. Importantly, we show that even minor modification of one of these parameters can have a dramatic impact on treatment outcome.

Treg-depletion increases BM $CD8^+$ T cell numbers and restores the efficacy of delayed anti-CD137 mAb treatment.

Our *in silico* analysis indicated that the suppressive effect of MM on $CD8^+$ T cells influences the outcome of anti-CD137 mAb treatment. This suppressive effect can be either direct or indirect, through the induction of immune-suppressive cells such as Tregs. A recent study indicated that Tregs' immunosuppressive functions were increased in MM (26). To assess whether Treg-mediated suppression impairs anti-CD137 mAb treatment efficacy, we first analyzed Treg responses during the course of anti-CD137 mAb treatment. We found that a single injection of anti-CD137 mAbs induced strong Treg proliferation in both tumor-naïve (Figure 9A) and MM-bearing mice (Supplemental Figure 9A). There was no difference in Treg numbers obtained following CD137-stimulation between week-2- and week-4-MM-bearing mice (Supplemental Figure 9B), suggesting that Treg responses to CD137 stimulation are similar at early and late disease stages. Next, we asked whether Tregs might impair CD137-mediated activation of T cells in MM-bearing mice. We took advantage of FoxP3-DTR mice in which Tregs are depleted by the injection of diphtheria toxin (DT) (27). At week 3 post Vk*MYC cell challenge, mice received a single DT injection followed by a single injection of anti-CD137 mAbs. We observed that DT injection alone increased $CD8^+$ T cell numbers in the BM as well as IFNγ production by both $CD4^+$ and $CD8^+$ T cells and this was further enhanced when mice received a combination of DT and anti-CD137 mAbs (Figures 9B-D and Supplemental Figure 9C). To determine the impact of Treg depletion on treatment efficacy, FoxP3-DTR mice were challenged with Vk*MYC cells and 3.5 weeks later, mice received a 2-week anti-CD137 mAb treatment combined with DT injections. At week 6 post MM-challenge, we observed a significant increase in BM $CD8^+$ T cell numbers in mice that received DT treatment alone or combined with anti-CD137 mAbs, but not in mice treated with single agent anti-CD137 mAbs (Supplemental Figure 9D). We observed a non-significant trend toward

decreased M-protein levels in mice treated with DT or anti-CD137 mAbs alone but only the combination of Treg-depletion with anti-CD137 mAbs significantly reduced monoclonal gammopathy and prolonged the survival of MM-challenged mice (Figures 9E and F). These results indicate that Treg-induced immunosuppression limits the efficacy of anti-CD137 mAb treatment. Therefore, we tested whether alleviating immunosuppression through checkpoint blockade could restore the efficacy of delayed anti-CD137 mAb treatment. However, in our hands, neither anti-PD-1 nor anti-CTLA-4 mAbs improved the anti-MM effect of delayed anti-CD137 mAb treatment (Supplemental Figures 9E and F). Taken as a whole, these data establish that efficient Treg depletion (but not PD-1 or CTLA-4 blockade) increases effector T cell-IFNγ response, expands BM $CD8^+$ T cells and improves the efficacy of anti-CD137 mAb therapy against MM.

Consolidation treatment with anti-CD137 mAbs following ~~cyclophosphamide administration~~ chemotherapy prolongs the survival of MM-bearing mice

We have established that tumor burden at the time of treatment is a determining factor for anti-CD137 mAb-efficacy. Thus, we investigated whether combination with cytotoxic agents that would "debulk" the tumor could restore the efficacy of delayed anti-CD137 mAb treatment. At week 3 post Vk*MYC cell challenge, mice were given an anti-CD137 mAb treatment combined with low-dose cyclophosphamide (20 mg/kg, Supplemental Figure 10A). However, this combination did not show improved efficacy when compared with anti-CD137 mAb treatment alone. This result may be explained by the inability of low-dose cyclophosphamide to significantly reduce the tumor burden and by its immune-suppressive effects leading to reduced $CD8^+$ T cell numbers (Supplemental Figures 10A and B). Therefore, we next tested a sequential treatment approach. Firstly, we tested whether anti-CD137 mAbs were effective when given after cyclophosphamide treatment. At week 3 post Vk*MYC cell challenge, two groups of mice were given 2 injections of 20 mg/kg of cyclophosphamide followed by a 2-week anti-CD137 mAb-treatment or IgG-control injections (Supplemental Figure 10C). ~~We observed that~~, Direct comparison between mice receiving cyclophosphamide only and mice receiving a sequential treatment of cyclophosphamide followed by anti-CD137 mAbs indicated that, when given after cyclophosphamide injections, delayed anti-CD137 mAb treatment led to increased numbers of BM $CD8^+$ T cells, associated with reduced tumor burden in the spleen and BM and reduced serum M-protein levels (Supplemental

Figure 10D-F). Then, we performed experiments with four groups of mice to include untreated and anti-CD137 mAbs single treatment, in addition to cyclophosphamide single treatment and sequential treatment. Interestingly, while injections of 25 mg/kg of cyclophosphamide on day 27 and 28 post MM injection failed to protect mice, improved survival was observed upon administration of subsequent anti-CD137 mAb treatment (Figures 10A and B). When given at higher doses (100 mg/kg), transient protection was observed with cyclophosphamide injections alone (Figure 10C). However, none of the mice receiving cyclophosphamide alone survived beyond day 100, in opposition to mice who received the sequential cyclophosphamide plus anti-CD137 mAb treatment (Figure 10D). Finally, we found that anti-CD137 mAbs improved disease control in mice that had been treated with melphalan, another chemotherapeutic commonly administered to MM patients (Figure 11). Altogether, these data emphasize the unique potential of immune stimulation through anti-CD137 mAbs to allow long-term survival and suggest that anti-CD137 mAbs might have better therapeutic effect when administered as a consolidation treatment following “debulking” therapy.

Discussion

Immune-based therapies hold promise for the treatment of MM (28). Still, the limited clinical activity of PD-1 checkpoint blockade as a single agent (5) and its toxicity when combined with IMiDs (6) emphasizes the need for better understanding of responses to immunotherapies in order to define the best timing and combination settings. In this study, we confirmed the high-therapeutic potential of anti-CD137 mAbs against MM while also demonstrating the limitations of this treatment. In the VK*MYC mouse model of MM, anti-CD137 mAb treatment failed to control advanced disease stages characterized by a high tumor burden and a decline in BM $CD8^+$ T cell numbers. We showed that releasing Treg-mediated immunosuppression or "debulking" the tumor through chemotherapy restores the efficacy of anti-CD137 mAb treatment at advanced disease stages.

Our data provide further insights on the mechanisms of action of anti-CD137 mAbs against MM. We previously established that, in the Vk*MYC model, anti-CD137 mAb therapy requires both $CD8^+$ T cells and NK cells (12). Here, we demonstrated that IFNγ also contributes to the anti-MM effect of anti-CD137 mAbs, a finding which is in agreement with observations made in other tumor models (29). IFNγ released in the context of anti-CD137 mAb therapy might either act directly on MM cells or might be necessary for the development of an efficient immune response. Our results suggest that both mechanisms contribute to the anti-MM effect of anti-CD137 mAbs. Indeed, MM grew faster in $IFN\gamma^{-/-}$ mice while tumor failed to develop in $IFN\gamma R^{-/-}$ mice. Given that VK*MYC cells express functional receptor to IFNγ (data not shown), these data indicate that excess of IFNγ in mice lacking its receptor directly inhibits MM cell engraftment in the BM. Interestingly, $CD8^+$ T cells were required for the protection of $IFN\gamma R^{-/-}$ mice against MM but $IFN\gamma R^{-/-}$ mice that had been depleted of $CD8^+$ T cells still exhibited increased levels of circulating IFNγ compared to WT mice (data not shown), demonstrating that high circulating levels of IFNγ are not sufficient to control MM in the absence of $CD8^+$ T cells. Moreover, $CD8^+$ T cell expansion following anti-CD137 mAb treatment was compromised in both $IFN\gamma^{-/-}$ and $IFN\gamma R^{-/-}$ mice, demonstrating that IFNγ signaling is required for the development of efficient $CD8^+$ T cell responses to anti-CD137 mAbs. We established that NK cells constitute the first lymphocyte subset to respond to CD137 stimulation. It is possible that early IFNγ-production by NK cells is a pre-requisite to $CD8^+$ T cell activation, as suggested by Wilcox et al. (30).

Although the experiments performed in the present study mostly focused on the IFNγ response induced by anti-CD137 mAbs, it should be noted that this therapy is also known for increasing T cell survival and cytotoxic activity (9). In our model, analysis of CD107a membrane expression indicated that both anti-CD137 mAb treatment and/or a high MM burden triggered $CD8^+$ T cell degranulation (data not shown). The observation of non–significant trend toward decreased MM burden in $IFN\gamma^{-/-}$ mice treated with anti-CD137 mAbs, indicates that IFNγ-independent mechanisms such as perforin/granzyme- or Fas-mediated killing of tumor cells probably contribute to the anti-MM effect of anti-CD137 mAbs.

We observed that NK cell responses to anti-CD137 mAbs were transient and that splenic NK cell numbers were dramatically reduced one week after the injection of anti-CD137 mAbs. Several explanations have been proposed for the anti-CD137 mAb-dependent loss of NK cells. Choi et al. suggested a block in NK cell development caused by IFNγ (22). However, in our hands, anti-CD137 mAb treatment depleted NK cells in both $IFN\gamma^{-/-}$ and $IFN\gamma R^{-/-}$ mice (data not shown). Niu et al. proposed that spleen NK cells traffic to the liver and lung in anti-CD137 mAb-treated mice (24) but we observed decreased NK cell numbers in both the lung and liver of MM-bearing mice treated with anti-CD137 mAbs (data not shown). The observation that anti-CD137 mAbs deplete NK cells in mice lacking activating Fc receptors (data not shown) ruled out the hypothesis of antibody dependent cellular cytotoxicity. It is possible that, in our system, NK cells undergo activation-induced cell death, as previously described (23).

The present study highlights the ability of MM cells to both induce and suppress immune responses. In mice with low MM burden, we established a positive correlation between the percentages of IFNγ-producing $CD8^+$ T cells and tumor burden, indicating that spontaneous $CD8^+$ T cell responses are triggered by the presence of MM cells. These data are in agreement with those from Dhodapkar et al. (31), who reported that T cells freshly isolated from the BM of patients diagnosed with monoclonal gammopathy of unknown significance (MGUS, the premalignant stage that precedes MM) are reactive against autologous premalignant cells. However, we found that, in mice with high MM burden, the correlation between IFNγ-producing $CD8^+$ T cells and tumor burden became negative. These data are in agreement with the observation that freshly isolated BM T cells from MM patients do not present any reactivity against autologous MM cancer cells (32), and suggest that, at advanced disease stages, the tumor becomes suppressive and inhibits the initially triggered spontaneous responses.

Given that immune responses are suppressed as MM grows, it is necessary to define the ability of immunotherapies to induce efficient immune responses in clinically active MM stages. Our data established that, even in mice with high tumor burden, T cells respond to CD137 stimulation by proliferating vigorously and secreting high amounts of IFNγ. This important information highlights the potential of anti-CD137 mAbs to reinvigorate T cell responses and to restore anti-tumor immunity even at advanced disease stages when T cells are actively repressed by the tumor. However, in this set of experiments T cell responses were investigated after a single injection of anti-CD137 mAbs and we have not ruled out the possibility that a 2-week anti-CD137 mAb treatment consisting of 4 injections may induce T cell exhaustion in advanced disease stages. In addition, several other hypotheses could explain why potent T cell responses to anti-CD137 mAbs did not translate into therapeutic activity in mice with high MM burden. We observed that the production of the immunosuppressive cytokine IL10 increases as MM grows, and this might contribute to repress T cell responses to anti-CD137 mAbs *in vivo*. Moreover, at advanced MM stages, we observed a drastic decline in total immune cell numbers in the BM (not shown). Notably, $CD8^+$ T cell numbers were dramatically reduced in mice with high MM burden prior to anti-CD137 mAb treatment and the fold increase in $CD8^+$ T cell numbers post-CD137 stimulation was lower at advanced disease stages. We propose that the lack of efficacy of anti-CD137 mAbs at late disease stages is due to the inability of this therapy to expand sufficient numbers of $CD8^+$ T cells, leading to an insufficient CD8/MM ratio.

Doban et al. (25) have proposed a dynamical model that considers the interactions between tumor cells, resting (i.e. naïve) and hunting (i.e. activated) immune cells through predator-prey competition terms. We adapted this model to fit our experimental data and study the interactions between $CD8^+$ T cells and MM cells in Vk*MYC cell-injected mice. Notably, we introduced a $CD8^+$ T cell contraction term associated with a new population of exhausted $CD8^+$ T cells; this was necessary for the system to return to steady-state conditions after eradication of the tumor. Moreover, we used delay differential equations (with discrete delays) to account for time-delays in $CD8^+$ T cell activation, $CD8^+$ T cell contraction and tumor dormancy. We also incorporated new parameters to distinguish between tumor-induced and immunotherapy-induced activation of $CD8^+$ T cells. This new model allowed us to evaluate the impact of various parameters (MM growth rate, $CD8^+$ T cell proliferation rate, $CD8^+$ T cell activation rate, $CD8^+$

T cell killing capacity, MM-immunosuppressive effect) on immunotherapy efficacy. We believe that the present model is suitable for the analysis of immune cell-tumor cell interactions in most cancer types and provides a useful tool for cancer immunologists.

We found that releasing immunosuppression through Treg-depletion increased BM $CD8^+$ T cell numbers and restored the efficacy of anti-CD137 mAbs against advanced MM disease. Although these findings suggest that immune-checkpoint blockade would be efficient in these settings, anti-CD137 mAb combination with anti-CTLA4 or anti-PD-1 mAbs did not show improved efficacy against advanced Vk*MYC MM tumors compared to anti-CD137 mAb as a single agent. These results are disappointing given the promising potential of combining CD137-stimulation with PD-1/PD-L1 blockade in solid tumors (33). Nevertheless, it was recently reported that PD-1 blockade abrogates the therapeutic efficacy of anti-CD137 mAbs in the Eμ-MYC model of mouse lymphoma (34). In agreement with this last report, our data emphasize the need for a better understanding of the underlying immune responses to combination therapies to define the specific cancer types and conditions where they might be beneficial. Moreover, we recently identified TIGIT as a dominant negative regulator of $CD8^+$ T cell responses against MM (35, 36). Since TIGIT is expressed at higher levels than PD-1 or CTLA-4 on BM $CD8^+$ T cells from MM patients (35), we suggest that combination of CD137 costimulation together with TIGIT blockade should be explored in MM.

We observed that anti-CD137 mAb treatment improved MM control when administered after chemotherapy with either cyclophosphamide or melphalan. Although low doses of cyclophosphamide are known for depleting Tregs (37), we observed no reduction in Treg numbers in the BM and spleen of mice treated with low dose cyclophosphamide (20 mg/kg). Since delayed anti-CD137 mAb treatment was also efficient after treatment with high dose cyclophosphamide or with the myeloablative agent melphalan, we do not think that modulation of Treg responses is instrumental for the success of sequential therapy. Instead, our data suggest that tumor ‘debulking’ leading to increased CD8/MM ratio is the main mechanism by which chemotherapy with cyclophosphamide or melphalan restores the efficacy of delayed anti-CD137 mAb treatment.

The identification of biomarkers of responses and the definition of optimal timing is of primary importance for the clinical development of immunotherapies. Here, we showed that M-protein measurement predicts response to anti-CD137 mAb immunotherapy. Therefore, we suggest that anti-CD137 mAbs should be administered to eradicate residual tumor cells after ‘debulking’ strategies. Accordingly, CD137 costimulation was found to promote long-term survival after autologous stem cell transplantation in the Vk*MYC MM model (38). Collectively, our data provide rationale for clinical trials to evaluate anti-CD137 mAbs as a consolidation treatment for MM patients with minimal residual disease.

Methods

Mice. All mice used in this study were on a C57BL/6 genetic background. C57BL/6 WT mice were purchased from the Walter and Eliza Hall Institute for Medical Research, bred in house at QIMR Berghofer Medical Research Institute or purchased from Janvier. C57BL/6, *Rag2*$^{-/-}$ *Il2rγ2*$^{-/-}$, *Ifnγ*$^{-/-}$, *Ifnγr*$^{-/-}$, *Ifnar*$^{-/-}$ and Foxp3-DTR mice have been previously described (12, 27, 39, 40). Mice were bred and maintained at QIMR Berghofer Medical Research Institute or in the SPF animal facility of the US006 CREFRE-Inserm/UPS, accredited by the French Ministry of Agriculture (accreditation number A-31 55508). Mice were used at 8-16 weeks of age. All experiments were approved by the QIMR Berghofer Medical Research Institute Animal Ethics Committee or by the local ethic committee (Midi-Pyrénées, France), in compliance with the French and European regulations on care and protection of laboratory animals.

Vk*MYC cell line model. All experiments have been performed with the Vk12653 Vk*MYC cell line as previously described (12). Briefly, Vk*MYC cells were expanded in *Rag2*$^{-/-}$*Il2rγ2*$^{-/-}$ mice and splenocytes from *Rag2*$^{-/-}$ *Il2rγ2*$^{-/-}$ mice containing 40-60% of malignant plasma cells were frozen down and used as a source of Vk*MYC MM cells. For Vk*MYC cell challenges, mice were injected i.v. with 2 x 10^6 live splenocytes from *Rag2*$^{-/-}$ *Il2rγ2*$^{-/-}$ mice. The presence of monoclonal Ig (M-protein; quantified as levels of γ-globulin) in the serum was determined by serum protein electrophoresis (HYDRASIS, Sebia Hydragel). In some experiments, the percentages and numbers of malignant plasma cells (MM cells) in the spleen and BM were analyzed by flow cytometry by gating on CD155$^+$CD138$^+$B220$^-$ live cells. For survival experiments, mice were monitored overtime for external signs of disease including back-leg paralysis, hunched posture, ruffled fur and swollen abdomen. Sick mice were sacrificed according to instructions from the QIMR Berghofer Medical Research Institute Animal Ethics Committee.

Anti-MM therapy. Mice receiving a 2-week anti-CD137 mAb treatment were injected i.p. with 100 µg of anti-CD137 mAbs (rat IgG2a, 3H3, BioxCell) or control rat IgG2a, twice a week for 2 weeks. In some experiments, mice received a single i.p. injection of 100 µg of anti-CD137 mAbs or control rat IgG2a.

To deplete Tregs, 250 ng of diphtheria toxin (DT; Sigma-Aldrich) were administered i.p. to C57BL/6 FoxP3-DTR mice, as previously described (27); control mice were injected with PBS.

Flow cytometry. Single-cell suspensions were resuspended in FACS buffer containing 2.4G2 (anti-CD16/32) to block Fc receptors. Cell surface staining was performed using the following conjugated mAbs: anti-mouse CD45.2 (104), TCRβ (H57-597), CD4 (RM4-5), CD8α (53-6.7), NK1.1 (PK136), NKp46 (29A1.4), B220 (RA3-6B2), CD138 (281-2), CD155 (4.24.1), CD62L (MEL-14), CD44 (IM7) and live/dead dye Zombie Yellow. For intracellular staining, cells were first surface stained and then fixed and permeabilized with Foxp3/Transcription Factor Fixation/Fixation kit (eBiosciences) and stained with anti-mouse FoxP3 (FJK-16s) or Ki67 (B56). Alternatively, to measure cytokine production, cells were first cultured for 2 hrs with PMA-ionomycin before being surface stained. Then cells were fixed and permeabilized with the BD Cytofix/Cytoperm kit (BD Biosciences) and stained with anti-mouse IFNγ (XMG1.2), TNF (MP6-XT22) or IL10 (JES5-16E3). All flow cytometry antibodies were purchased from BioLegend or eBioscience. BD Liquid Counting Beads (BD Biosciences) were added to each sample to determine cell numbers. Samples were acquired on an LSR Fortessa 4 lasers flow cytometer (BD Biosciences) and analyzed with FlowJo v10 (Tree Star).

Statistical analyses. Statistical analyses were carried out using the GraphPad Prism Software except for the logistic regression and partition tree which were performed using JMP Pro v 14 (SAS institute. Cary NC). For data presented on a log-scale (MM or T cell numbers), statistical analyses were performed on the log-transformed data with the indicated test. Two-sample analyses were performed using a Mann-Whitney U test. Group analyses were performed with a Kruskal-Wallis test followed by a Dunn's multiple comparison post-hoc test. The log-rank test was used for survival analyses. The Pearson r correlation coefficient was calculated to assess correlation between 2 parameters, except for Figure 5C where data were analyzed with an unconstrained segmental regression using the GraphPad Prism software.

Author contributions

Study conception and design: C.G. and M.J.S. Acquisition of data: C.G., A.C.P., S.K., K.S., K.M., K.N., H.H., M.C. and Y.Y. Analysis and interpretation of data: C.G., K.N., A.C.P, D.B., L.M. and M.J.S. Statistical analyses: G.H. and D.S. *In silico* analyses: C.G., D.B., A.I.D. and M.L. Drafting of the manuscript: C.G. Critical revision and editing: D.B., K.N., S.V., M.W.L.T., P.L.B., M.C., G.R.H. and M.J.S. Supervision: M.W.L.T., G.R.H., L.M. and M.J.S.

Acknowledgments

The authors thank Liam Town and Kate Elder for breeding, genotyping, maintenance, and care of the mice used in this study. We thank the animal house and flow cytometry facilities at QIMR Berghofer Medical Research Institute; and members of Immunology in Cancer and Infection Laboratory, members of the Cancer Immunoregulation and Immunotherapy Laboratory and members of the Bone Marrow Transplantation Laboratory as well as Christian Engwerda for helpful suggestions and discussion. We thank Kestutis Barkauskas for his precious help in developing the *in silico* model. This work was funded by a Project grant from Cure Cancer Australia, Cancer Australia and Can Too (1122183) and a QIMR Berghofer Seed Grant to C.G., and by a NH&MRC Program Grant (1132519) and Project Grant (1098960) to M.J.S. and M.W.L.T. C.G. was supported by a National Health and Medical Research Council (NHMRC) of Australia Early Career Fellowship (1107417). A.C.P. was supported by a grant from "Ligue nationale contre le cancer". H.H. was supported by a UQ International Postgraduate Research Scholarship, a UQ Australian Postgraduate Award and QIMR Berghofer Top-Up awards. K.N. was supported by the Naito Foundation. G. R.H. was supported by a NHMRC Program Grant (1071822) and Research Fellowship (1107797). M. J. S. was supported by a Senior Principal Research Fellowship (1078671).

References

1. Kumar SK, Rajkumar V, Kyle RA, van Duin M, Sonneveld P, Mateos MV, et al. Multiple myeloma. *Nat Rev Dis Primers.* 2017;3:17046.
2. Rasche L, Weinhold N, Morgan GJ, van Rhee F, and Davies FE. Immunologic approaches for the treatment of multiple myeloma. *Cancer Treat Rev.* 2017;55:190-9.
3. Touzeau C, Moreau P, and Dumontet C. Monoclonal antibody therapy in multiple myeloma. *Leukemia.* 2017;31(5):1039-47.
4. D'Agostino M, Boccadoro M, and Smith EL. Novel Immunotherapies for Multiple Myeloma. *Curr Hematol Malig Rep.* 2017.
5. Rosenblatt J, and Avigan D. Targeting the PD-1/PD-L1 axis in multiple myeloma: a dream or a reality? *Blood.* 2017;129(3):275-9.
6. Badros A, Hyjek E, Ma N, Lesokhin A, Dogan A, Rapoport AP, et al. Pembrolizumab, pomalidomide, and low-dose dexamethasone for relapsed/refractory multiple myeloma. *Blood.* 2017;130(10):1189-97.
7. Sanmamed MF, Pastor F, Rodriguez A, Perez-Gracia JL, Rodriguez-Ruiz ME, Jure-Kunkel M, et al. Agonists of Co-stimulation in Cancer Immunotherapy Directed Against CD137, OX40, GITR, CD27, CD28, and ICOS. *Semin Oncol.* 2015;42(4):640-55.
8. Bartkowiak T, and Curran MA. 4-1BB Agonists: Multi-Potent Potentiators of Tumor Immunity. *Front Oncol.* 2015;5:117.
9. Chester C, Sanmamed MF, Wang J, and Melero I. Immunotherapy targeting 4-1BB: mechanistic rationale, clinical results, and future strategies. *Blood.* 2018;131(1):49-57.
10. Teijeira A, Labiano S, Garasa S, Etxeberria I, Santamaria E, Rouzaut A, et al. Mitochondrial Morphological and Functional Reprogramming Following CD137 (4-1BB) Costimulation. *Cancer Immunol Res.* 2018;6(7):798-811.
11. Aznar MA, Labiano S, Diaz-Lagares A, Molina C, Garasa S, Azpilikueta A, et al. CD137 (4-1BB) Costimulation Modifies DNA Methylation in CD8(+) T Cell-Relevant Genes. *Cancer Immunol Res.* 2018;6(1):69-78.
12. Guillerey C, Ferrari de Andrade L, Vuckovic S, Miles K, Ngiow SF, Yong MC, et al. Immunosurveillance and therapy of multiple myeloma are CD226 dependent. *J Clin Invest.* 2015;125(5):2077-89.
13. Murillo O, Arina A, Hervas-Stubbs S, Gupta A, McCluskey B, Dubrot J, et al. Therapeutic antitumor efficacy of anti-CD137 agonistic monoclonal antibody in mouse models of myeloma. *Clin Cancer Res.* 2008;14(21):6895-906.
14. Makkouk A, Chester C, and Kohrt HE. Rationale for anti-CD137 cancer immunotherapy. *Eur J Cancer.* 2016;54:112-9.
15. Sanchez-Paulete AR, Cueto FJ, Martinez-Lopez M, Labiano S, Morales-Kastresana A, Rodriguez-Ruiz ME, et al. Cancer Immunotherapy with Immunomodulatory Anti-CD137 and Anti-PD-1 Monoclonal Antibodies Requires BATF3-Dependent Dendritic Cells. *Cancer Discov.* 2016;6(1):71-9.
16. Segal NH, Logan TF, Hodi FS, McDermott D, Melero I, Hamid O, et al. Results from an Integrated Safety Analysis of Urelumab, an Agonist Anti-CD137 Monoclonal Antibody. *Clin Cancer Res.* 2017;23(8):1929-36.
17. Tolcher AW, Sznol M, Hu-Lieskovan S, Papadopoulos KP, Patnaik A, Rasco DW, et al. Phase Ib Study of Utomilumab (PF-05082566), a 4-1BB/CD137 Agonist, in Combination with Pembrolizumab (MK-3475) in Patients with Advanced Solid Tumors. *Clin Cancer Res.* 2017;23(18):5349-57.
18. Segal NH, He AR, Doi T, Levy R, Bhatia S, Pishvaian MJ, et al. Phase I Study of Single-Agent Utomilumab (PF-05082566), a 4-1BB/CD137 Agonist, in Patients with Advanced Cancer. *Clin Cancer Res.* 2018;24(8):1816-23.

19. Guillerey C, Nakamura K, Vuckovic S, Hill GR, and Smyth MJ. Immune responses in multiple myeloma: role of the natural immune surveillance and potential of immunotherapies. *Cell Mol Life Sci.* 2016;73(8):1569-89.
20. Dosani T, Mailankody S, Korde N, Manasanch E, Bhutani M, Tageja N, et al. Host-related immunodeficiency in the development of multiple myeloma. *Leuk Lymphoma.* 2017:1-6.
21. Ascierto PA, Simeone E, Sznol M, Fu YX, and Melero I. Clinical experiences with anti-CD137 and anti-PD1 therapeutic antibodies. *Semin Oncol.* 2010;37(5):508-16.
22. Choi BK, Kim YH, Kim CH, Kim MS, Kim KH, Oh HS, et al. Peripheral 4-1BB signaling negatively regulates NK cell development through IFN-gamma. *J Immunol.* 2010;185(3):1404-11.
23. Lee SW, Salek-Ardakani S, Mittler RS, and Croft M. Hypercostimulation through 4-1BB distorts homeostasis of immune cells. *J Immunol.* 2009;182(11):6753-62.
24. Niu L, Strahotin S, Hewes B, Zhang B, Zhang Y, Archer D, et al. Cytokine-mediated disruption of lymphocyte trafficking, hemopoiesis, and induction of lymphopenia, anemia, and thrombocytopenia in anti-CD137-treated mice. *J Immunol.* 2007;178(7):4194-213.
25. Doban AI, and Lazar M. A switching control law approach for cancer immunotherapy of an evolutionary tumor growth model. *Math Biosci.* 2017;284:40-50.
26. Kawano Y, Zavidij O, Park J, Moschetta M, Kokubun K, Mouhieddine TH, et al. Blocking IFNAR1 inhibits multiple myeloma-driven Treg expansion and immunosuppression. *J Clin Invest.* 2018;128(6):2487-99.
27. Liu J, Blake SJ, Harjunpaa H, Fairfax KA, Yong MC, Allen S, et al. Assessing Immune-Related Adverse Events of Efficacious Combination Immunotherapies in Preclinical Models of Cancer. *Cancer Res.* 2016;76(18):5288-301.
28. Kohler M, Greil C, Hudecek M, Lonial S, Raje N, Wasch R, et al. Current developments in immunotherapy in the treatment of multiple myeloma. *Cancer.* 2018;124(10):2075-85.
29. Wilcox RA, Flies DB, Wang H, Tamada K, Johnson AJ, Pease LR, et al. Impaired infiltration of tumor-specific cytolytic T cells in the absence of interferon-gamma despite their normal maturation in lymphoid organs during CD137 monoclonal antibody therapy. *Cancer Res.* 2002;62(15):4413-8.
30. Wilcox RA, Tamada K, Strome SE, and Chen L. Signaling through NK cell-associated CD137 promotes both helper function for CD8+ cytolytic T cells and responsiveness to IL-2 but not cytolytic activity. *J Immunol.* 2002;169(8):4230-6.
31. Dhodapkar MV, Krasovsky J, Osman K, and Geller MD. Vigorous premalignancy-specific effector T cell response in the bone marrow of patients with monoclonal gammopathy. *J Exp Med.* 2003;198(11):1753-7.
32. Dhodapkar MV, Krasovsky J, and Olson K. T cells from the tumor microenvironment of patients with progressive myeloma can generate strong, tumor-specific cytolytic responses to autologous, tumor-loaded dendritic cells. *Proc Natl Acad Sci U S A.* 2002;99(20):13009-13.
33. Perez-Ruiz E, Etxeberria I, Rodriguez-Ruiz ME, and Melero I. Anti-CD137 and PD-1/PD-L1 Antibodies En Route toward Clinical Synergy. *Clin Cancer Res.* 2017;23(18):5326-8.
34. McKee SJ, Doff BL, Soon MS, and Mattarollo SR. Therapeutic Efficacy of 4-1BB Costimulation Is Abrogated by PD-1 Blockade in a Model of Spontaneous B-cell Lymphoma. *Cancer Immunol Res.* 2017;5(3):191-7.
35. Guillerey C, Harjunpaa H, Carrie N, Kassem S, Teo T, Miles K, et al. TIGIT immune checkpoint blockade restores CD8(+) T cell immunity against multiple myeloma. *Blood.* 2018.
36. Minnie SA, Kuns RD, Gartlan KH, Zhang P, Wilkinson AN, Samson L, et al. Myeloma-escape after stem cell transplantation is a consequence of T cell exhaustion and is prevented by TIGIT blockade. *Blood.* 2018.
37. Ahlmann M, and Hempel G. The effect of cyclophosphamide on the immune system: implications for clinical cancer therapy. *Cancer Chemother Pharmacol.* 2016;78(4):661-71.
38. Vuckovic S, Minnie SA, Smith D, Gartlan KH, Watkins TS, Markey KA, et al. Bone marrow transplantation generates T cell-dependent control of myeloma in mice. *J Clin Invest.* 2018.

39. Starr R, Fuchsberger M, Lau LS, Uldrich AP, Goradia A, Willson TA, et al. SOCS-1 binding to tyrosine 441 of IFN-gamma receptor subunit 1 contributes to the attenuation of IFN-gamma signaling in vivo. *J Immunol.* 2009;183(7):4537-44.
40. Hwang SY, Hertzog PJ, Holland KA, Sumarsono SH, Tymms MJ, Hamilton JA, et al. A null mutation in the gene encoding a type I interferon receptor component eliminates antiproliferative and antiviral responses to interferons alpha and beta and alters macrophage responses. *Proc Natl Acad Sci U S A.* 1995;92(24):11284-8.

Figure legends

Figure 1: Early anti-CD137 mAb treatment increases T cell numbers and provides long term protection against MM. C57BL/6 WT mice were challenged iv with 2 x 10^6 Vk12653 (Vk*MYC) cells and after 2 weeks, mice received a 2-week anti-CD137 mAb treatment or control rat IgG2a (IgG). (A) Survival was monitored over time. Data were pooled from 2 independent experiments, each with n=9-10 mice per group and analyzed with a Log-rank test ($p < 0.0001$). (B) Representative serum electrophoresis gel at week 5 post Vk*MYC cell challenge. Arrows indicate the M-protein bands. (C-E) Numbers of (C) malignant $CD155^+$ plasma cells (MM cells), (D) $CD8^+$ T cells and (E) $FoxP3^-$ $CD4^+$ T helper cells (Th) in the spleen and BM were determined by flow cytometry at week 5 post Vk*MYC cell challenge. Graphs show geometric mean ± SD of one experiment (n=7-10 mice per group) representative of 2 independent experiments. Statistical differences were assessed with a Mann-Whitney U test. * $p < 0.05$; ** $p < 0.01$; *** $p < 0.001$; **** $p < 0.0001$.

Figure 2: Anti-CD137 mAb treatment induces potent effector memory T cell responses. WT mice were challenged with Vk*MYC cells and after 3 weeks, mice received a 2-week anti-CD137 mAb treatment. (A) BM and (B) spleen cells were isolated at week 5 post-Vk*MYC cell challenge, cultured with PMA-ionomycin for 2 hrs and IFN-γ, TNF and IL-10 production by CD4 and CD8 T cells was determined by intracellular staining. Graphs show mean ± SEM of one experiment (n=9-10 mice per group) representative of 2 independent experiments. Statistical differences were assessed with a Mann-Whitney U test. * $p < 0.05$; ** $p < 0.01$; *** $p < 0.001$; **** $p < 0.0001$. (C) Naïve WT mice received a 2 week anti-CD137 mAb treatment and the percentages of naïve ($CD62L^+CD44^-$), effector/effector-memory (TEM: $CD62L^-CD44^+$) or central memory (TCM: $CD62L^+CD44^+$) BM $CD8^+$ T cells were analyzed by flow cytometry. Data are shown as representative graph plots (left) and pie-charts (right) displaying mean ± SD of 4 independent experiments, each with n=2-4 mice per group.

Figure 3: NK cells and T cells show different kinetics of response to CD137 stimulation. Naïve WT mice received a single ip injection of 100 µg of anti-CD137 mAbs or control IgG on day 0 and analysis was performed on day 1, 3 and 7. (A, B) Proliferation of BM NK cells (NK), $FoxP3^-$ $CD4^+$ T cells

(CD4 Th) and $CD8^+$ T cells (CD8) was assessed by Ki67 staining. (C, D) Total BM cells were cultured with PMA-ionomycin for 2 hrs and IFN-γ production by NK cells, $CD4^+$ T cells (CD4) and $CD8^+$ T cells was assessed by intracellular staining. (E, F) NK cell numbers in the spleen and BM were quantified by flow cytometry. Data are shown as (A, C, E) representative staining on day 7 or (B, D, F) mean ± SEM of data from 2 pooled experiments, each with n=5 mice per group. Dot-plots in E are from the spleen. Data were analyzed with a Kruskal-Wallis test followed by a Dunn's multiple comparisons post-hoc test. * $p < 0.05$; ** $p < 0.01$; *** $p < 0.001$.

Figure 4: IFNγ signaling is required for optimal efficacy of anti-CD137 mAb therapy. (A) Naïve WT, *Ifnγ*$^{-/-}$ or *Ifnγr*$^{-/-}$ mice received a 2-week anti-CD137 mAb treatment and $CD8^+$ T cell numbers in the spleen were determined by flow cytometry. The geometric means ± SD of 4 pooled experiments (each with 3-4 mice per group) are shown. Data acquired within the same experiment are depicted with similar symbols. (B-E) WT or *Ifnγ*$^{-/-}$ were challenged with Vk*MYC cells and 2 weeks later, mice received a 2-week anti-CD137 mAb treatment. At week 5 post Vk*MYC cell challenge, numbers of BM (B left) or spleen (B right) MM cells as well as (C) percentages of $CD8^+$ T cells within BM lymphocytes were analyzed by flow cytometry. (D-E) Total BM cells were cultured with PMA-ionomycin for 2 hrs and IL10 production by $CD4^+$ T cells was determined by intracellular staining. Graphs show (B) geometric mean ± SD or (E) mean ± SEM of 1 experiment with n = 9-11 mice per group. Data were analyzed with (A) a Mann-Whitney U test or (B, E) a Kruskal-Wallis test followed by a Dunn's multiple comparison post hoc test. * $p < 0.05$; ** $p < 0.01$, *** $p < 0.001$, ns: non significant.

Figure 5: MM growth is associated with progressive immunosuppression and loss of anti-CD137 mAb treatment efficacy. (A-B) WT mice were challenged with Vk*MYC cells and mice received a 2-week anti-CD137 mAb treatment starting from week 1, 2, 3 or 4 post Vk*MYC cell challenge (see Supplemental Figure 5C). (A) Tumor burden in the BM (left) or the spleen (right) was analyzed by flow cytometry at week 6 post Vk*MYC cell challenge. (B) Monoclonal gammopathy was analyzed over time by serum electrophoresis. Graphs display (A) the geometric mean ± SD or (B) mean ± SEM of 1 experiment with n = 9-10 mice per group. Data were analyzed with a Kruskal-Wallis test followed by a Dunn's multiple comparisons post-hoc test performed on week 6 values. * $p < 0.05$; ** $p < 0.01$; **** p

< 0.0001, ns: non significant. (C-D) WT mice were challenged with Vk*MYC cells and 3 to 6 weeks later, BM cells were collected and cultured with PMA-ionomycin for 2 hrs. (C) IFNγ-production by $CD8^+$ T cells or (D) IL10-production by $CD4^+$ and $CD8^+$ T cells were measured by intracellular staining. Data are pooled from n=9-10 independent experiments with a total of n=76-91 mice that have either been left untreated or received control treatment (PBS or IgG). (C) Data were analyzed with the GraphPad Prism software using unconstrained segmental linear regression, $p < 0.0001$; X0 = 479425. (D) Data were analyzed with a Pearson correlation test.

Figure 6: In mice with high MM burden, T cells are responsive to CD137 stimulation but delayed anti-CD137 mAb treatment fails to expand large numbers of $CD8^+$ T cells. (A-C) WT mice received a single injection of anti-CD137 mAbs at week 2 or 4 post Vk*MYC cell challenge. T cell responses in the BM were analyzed 1 week later. Naïve mice were used as control. (A) Proliferation of $CD4^+$ Th ($FoxP3^-$) and $CD8^+$ T cells was assessed by intracellular Ki67 staining. (B) IFNγ-production by $CD4^+$ and $CD8^+$ T cells was assessed by intracellular staining. (C) $CD8^+$ T cell numbers in the BM were determined by flow cytometry. (D-E) WT mice were challenged with Vk*MYC cells (close circles) and 1 to 6 weeks later, numbers of CD8 T cell and MM cells in the BM were analyzed by flow-cytometry. (D) $CD8^+$ T cells in the BM of naïve mice were analyzed as control (open squares) and have been attributed the value of 1 MM cell to be plotted on the log axis. (E) The ratio between $CD8^+$ T cells and tumor cells (CD8/MM ratio) was determined by flow cytometry at different time points. The color rectangles highlight data at time points when anti-CD137 mAb treatment generally decreases tumor growth in most of the mice (green), decreases tumor growth in only some mice (orange) or has no effect on tumor growth in most of the mice (red). Data are pooled from (A-C) n=2 independent experiments, each with n=3-5 mice per group, (D-E) n=16 independent experiments with n=60 naïve and n=171 MM-bearing mice. Data were analyzed with (A-C) a Mann-Whitney U test or (E) a Pearson correlation test, * $p < 0.05$; *** $p < 0.001$; **** $p < 0.0001$.

Figure 7: Initial MM burden determines treatment efficacy. (A-B) WT mice were challenged with Vk*MYC cells and 2-4 weeks later, serum M-protein levels were measured before the mice were given a 2 week anti-CD137 mAb treatment. Mice were categorized as responders if their serum M-protein

levels after treatment were below 30 %. Data from 3 independent experiments with a total of n= 30 mice was analyzed. (A) Logistic fit (left) and corresponding confusion matrix (right) of the probability to be a non-responder versus pre-treatment M-protein levels (likelihood ratio $\chi_1^2 = 19.0$, P<0.0001). According to this analysis, mice with pre-treatment M-protein levels of 13.61 % (95% CI 7.34, 29.37) have a 50 % chance to respond to the treatment. (B) Partition tree classifying mice with pre-treatment M-protein levels < 10.2 % as responders and others as non responders.

Figure 8: Modeling interactions between CD8⁺ T cells and MM cells in the context of anti-CD137 mAb treatment. Dynamic interactions between MM cells and CD8⁺ T cells were modeled *in silico.* (A) Numbers of MM cells and naïve, activated and exhausted CD8⁺ T cells overtime using optimized parameters to fit the experimental data in untreated mice. (B-C) Effect of a 2-week anti-CD137 mAb started at different time points between day 7 and 28 post MM injection. (B) Graphs within a column represent the numbers of MM cells and total CD8 T cells overtime when treatment was started on a given day post MM injection (indicated at the top of each column). (C) Scale from graphs in B was adjusted to visualize the evolution of MM cell numbers when treatment was efficient.

Figure 9: Treg-depletion promotes the expansion of IFNγ-producing CD8⁺ T cells in the BM and restores the efficacy of delayed anti-CD137 mAb treatment. (A) WT mice received a single anti-CD137 mAb injection on day 0 and FoxP3⁺ Treg proliferation was analyzed on day 1, 3 and 7. (B-D) FoxP3-DTR mice were challenged with Vk*MYC cells on day 0 and were given 250 ng of DT (or PBS as control) on day 21, and a single injection of anti-CD137 mAbs (or control IgG) on day 22. BM T cells were analyzed by flow cytometry on day 28. (B) CD8⁺ T cell percentages, gated on live CD45.2⁺ lymphocytes. (C) Percentages of IFNγ⁺ CD4⁺ and CD8⁺ T cells. (D) Quantification of IFNγ⁺ CD8⁺ T cell numbers. (E-F) FoxP3-DTR mice were challenged with Vk*MYC cells on day 0. Mice received 250 ng of DT on day 24 and 29, together with a 2-week anti-CD137 mAb treatment from day 25. (E) At the end of the treatment, serum M-protein levels were determined by electrophoresis. Numbers indicate the number of mice excluded (that had already succumbed to MM) over the total number of mice per group. (F) Survival was followed overtime. Data are (A-C) representative or shown as (D) geometric mean ± SD or (E) mean ± SEM of 2 experiments, each with n=5-10 mice per group. Symbol shapes identify

data from independent experiments. (F) Data are from 1 experiment with n = 6-10 mice per group. Data were analyzed using (D-E) a Kruskal-Wallis test followed by a Dunn's multiple comparison post-hoc test or (H) a Log-rank test, *p < 0.05; ** p < 0. 01; *** p < 0. 001; **** p < 0.0001.

Figure 10: Anti-CD137 mAb treatment prevents relapse after cyclophosphamide treatment and allows long-term survival. C57BL/6 WT mice were challenged with Vk*MYC cells on day 0. Four weeks later, mice received a treatment consisting of 2 injections of cyclophosphamide (CP) followed by 2-week anti-CD137 mAb treatment (as explained in Supplemental Figure 10C). (A, B) Mice were injected with 25 mg/kg of CP on day 27 and 28. (A) Survival was monitored overtime. (B) Serum electrophoresis was performed on day 26 (before treatment) and on day 41 (2 weeks after the treatment started). Variation in γ-globulin levels between these 2 time points is displayed as mean ± SEM. Data are from one experiment with n=8-10 mice per group. (C) Mice were injected with 100 mg/kg of CP on day 28 and 29. Data are combined from 2 independent experiments with n=11-15 mice per group (D) Data from panel A (Experiment 1) and panel C (Experiments 2 and 3) are shown as percentages of mice alive on day 50, 70 and 100. Numbers at the top of each bar indicate the absolute number of mice alive at a given time point. The mean percentages of surviving mice within each group are indicated. Data were analyzed with a Log-rank test (A, C) or with a Kruskal-Wallis test (B). * p < 0.05; *** p < 0.001; **** p < 0.0001.

Figure 11: Sequential therapy with melphalan injections followed by anti-CD137 mAb treatment improves disease control. C57BL/6 WT mice were challenged with Vk*MYC cells on day 0. On day 21 and 22, mice were injected i.p. with 4 mg/kg of melphalan (Mel). Mice received a 2-week anti-CD137 mAb treatment starting from day 25. On day 45, (A) serum levels of γ-globulin (M-protein) were analyzed by electrophoresis (B) percentages of MM cells in the BM were determined by flow cytometry. Data are shown as mean ± SEM of 2 experiments, each with 6-8 mice per group. Symbol shapes identify data from independent experiments. Data were analyzed with Kruskal-Wallis test followed by a Dunn's multiple comparison post-hoc test. * p < 0.05; ** p < 0.01.

Parameter	Value of the modified parameter	Time (T_{lim})when the treatment no longer eradicates the tumor (days)	MM cell numbers at T_{lim}	Total $CD8^+$ T cell numbers at T_{lim}	Activated $CD8^+$ T cell numbers at T_{lim}	Ratio Total CD8/MM at T_{lim}	Ratio Activated CD8/MM at T_{lim}
Starting number of MM cells (i.e. number of MM cells reaching 1 femur)	19295	34	403717	284635	43757	0.71	0.11
	20000	26	389569	269031	46704	0.69	0.12
	21000	**25**	**360933**	**268938**	**46223**	**0.75**	**0.13**
	22000	24	337088	268468	45679	0.80	0.14
	23000	23	312781	267544	45226	0.86	0.14
	24000	23	296769	266020	44412	0.90	0.15
	25000	22	278684	264195	43834	0.95	0.16
	50000	18	387572	217914	37032	0.56	0.10
	100000	14	440246	176642	37441	0.40	0.09
Fitted value:	500000	5	494804	128816	11608	0.26	0.02
21 000	1000000	1	998843	144492	14587	0.14	0.01
Growth Rate of the MM cells (R_M)	0.18	42	436078	344955	33029	0.79	0.08
	0.2	35	390557	318888	33747	0.82	0.09
	0.25	30	446560	295064	38984	0.66	0.09
	0.3	27	427168	281024	43924	0.66	0.10
	0.35	**25**	**360933**	**268938**	**46223**	**0.75**	**0.13**
	0.5	20	207649	244304	45212	1.18	0.22
Fitted value : 0.35	1	17	364732	220417	41604	0.60	0.11
	2	15	502561	207402	47524	0.41	0.09
	5	11	341400	191310	61290	0.56	0.18
Suppressive effect of the MM cells on activated $CD8^+$ T cells (σ_A)	0.03	30	708163	335116	71671	0.47	0.10
	0.04	27	520800	297450	58145	0.57	0.11
	0.05	**25**	**360933**	**268938**	**46223**	**0.75**	**0.13**
	0.06	23	228180	248927	35998	1.09	0.16
	0.07	21	169663	235887	29282	1.39	0.17
Fitted value: 0.05	0.1	19	168762	212766	17589	1.26	0.10
Suppressive effect of the MM cells on naive $CD8^+$ T cells (σ_Z)	0	25	418586	339894	46310	0.81	0.11
	0.0001	25	418625	338927	46277	0.81	0.11
	0.001	25	411226	329734	46078	0.80	0.11
	0.01	**25**	**360933**	**268938**	**46223**	**0.75**	**0.13**
	0.1	24	294140	188722	45112	0.64	0.15
Fitted value: 0.01	1	24	312977	187503	45018	0.60	0.14
Killing capacity of activated $CD8^+$ T cells during treatment (γ)	0.08	8	9783	166394	37342	17.01	3.82
	0.1	9	6340	175319	44253	27.65	6.98
	0.5	18	134923	234922	63878	1.74	0.47
	1	20	144561	250373	57532	1.73	0.40
	2	23	234604	265356	50578	1.13	0.22
	3	25	405878	269182	44063	0.66	0.11
Fitted value: 2.7	5	27	598287	266904	33228	0.45	0.06
	8	29	750472	260476	24300	0.35	0.03
	10	29	795583	256642	21208	0.32	0.03

Table 1: **Influence of different parameters on the ability of anti-CD137 mAb treatment to eliminate MM cells.** Fitted values for each parameter were determined to best fit our experimental observations and were kept constant as different values for each parameter were tested individually to determine their influence on the $CD8^+$ T cells - MM cells dynamics within the system.

Figure 1

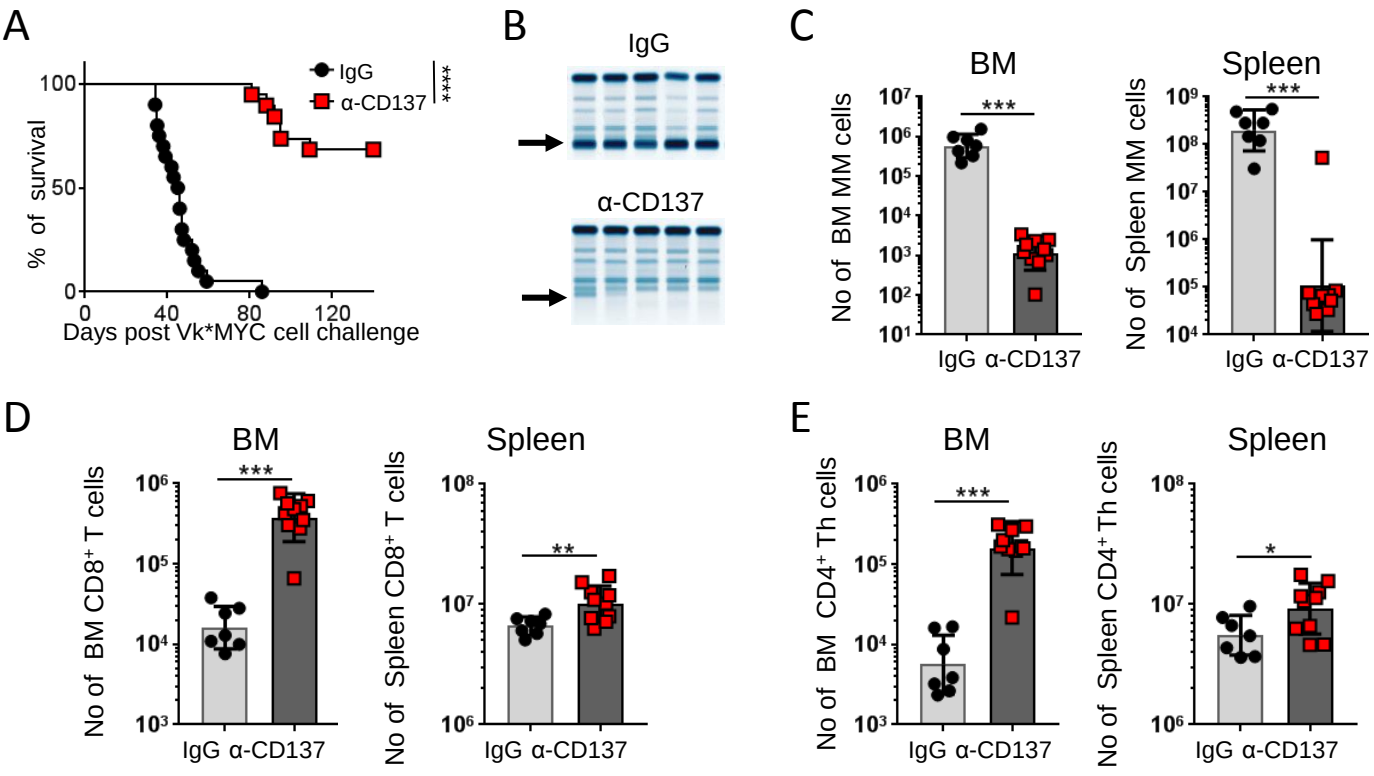

Figure 1: Early anti-CD137 mAb treatment increases T cell numbers and provides long term protection against MM.

C57BL/6 WT mice were challenged iv with 2 x 10^6 Vk12653 (Vk*MYC) cells and after 2 weeks, mice received a 2-week anti-CD137 mAb treatment. (A) Survival was monitored over time. Data were pooled from 2 independent experiments, each with n=9-10 mice per group and analyzed with a Log-rank test ($p < 0.0001$). (B) Representative serum electrophoresis gel at week 5 post Vk*MYC cell challenge. Arrows indicate the M-protein bands. (C-E) Numbers of (C) malignant $CD155^+$ plasma cells (MM cells), (D) $CD8^+$ T cells and (E) $FoxP3^-$ $CD4^+$ helper T cells (Th) in the spleen and BM were determined by flow cytometry at week 5 post Vk*MYC cell challenge. Graphs show geometric mean ± SD of one experiment (n=7-10 mice per group) representative of 2 independent experiments. Statistical differences were assessed with a Mann-Whitney U test. * $p < 0.05$; ** $p < 0.01$; *** $p < 0.001$; **** $p < 0.0001$.

Figure 2

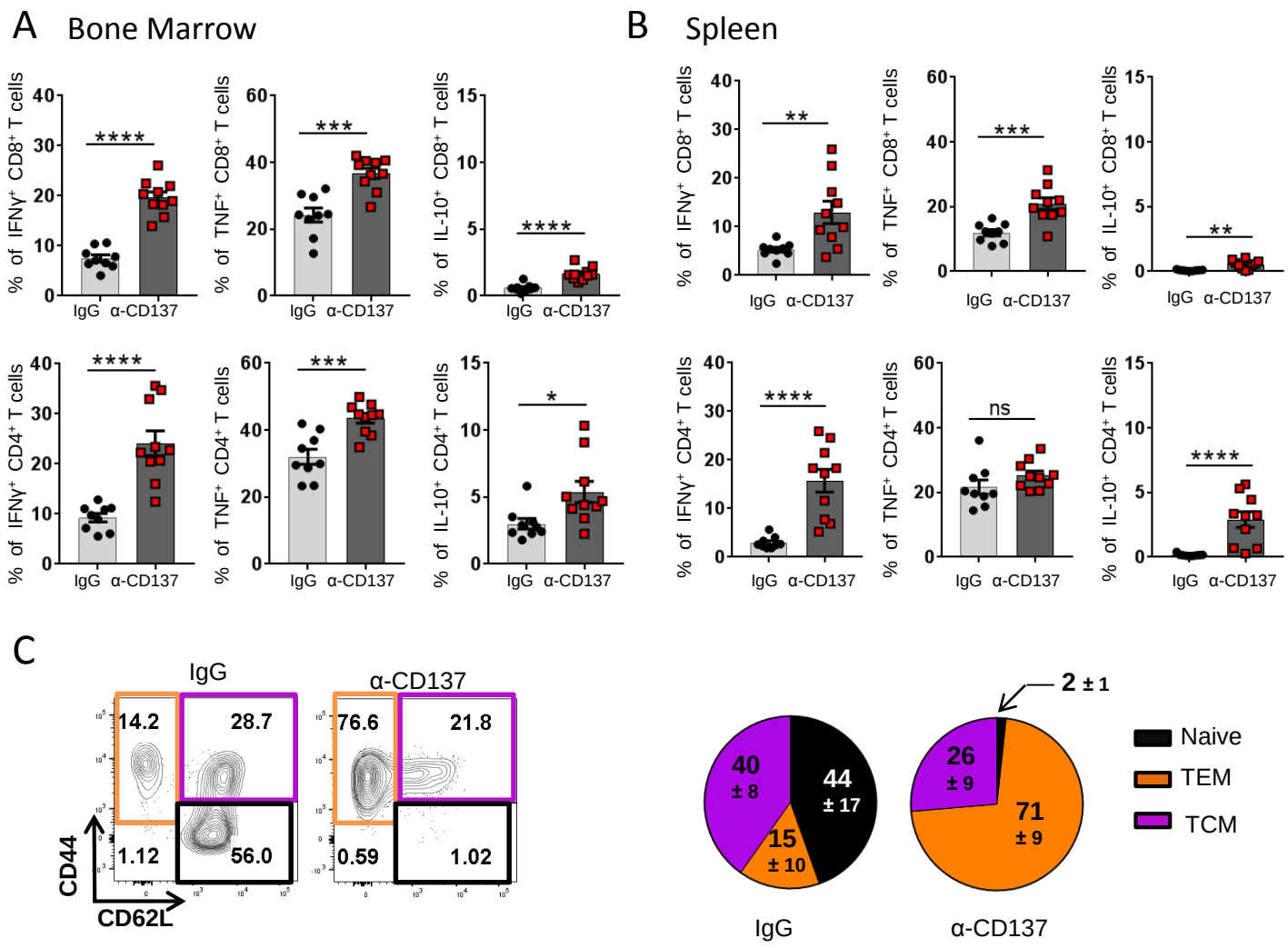

Figure 2: Anti-CD137 mAb treatment induces potent effector memory T cell responses.
WT mice were challenged with Vk*MYC cells and after 3 weeks, mice received a 2-week anti-CD137 mAb treatment. (A) BM and (B) spleen cells were isolated at week 5 post-Vk*MYC cell challenge, cultured with PMA-ionomycin for 2 hrs and IFN-γ, TNF and IL-10 production by CD4 and CD8 T cells was determined by intracellular staining. Graphs show mean ± SEM of one experiment (n=9-10 mice per group) representative of 2 independent experiments. Statistical differences were assessed with a Mann-Whitney U test. * $p < 0.05$; ** $p < 0.01$; *** $p < 0.001$; **** $p < 0.0001$. (C) Naïve WT mice received a 2 week anti-CD137 mAb treatment and the percentages of naïve ($CD62L^+CD44^-$), effector/effector-memory (TEM: $CD62L^-CD44^+$) or central memory (TCM: $CD62L^+CD44^+$) BM $CD8^+$ T cells were analyzed by flow cytometry. Data are shown as representative graph plots (left) and pie-charts (right) displaying mean ± SD of 4 independent experiments, each with n=2-4 mice per group.

Figure 3

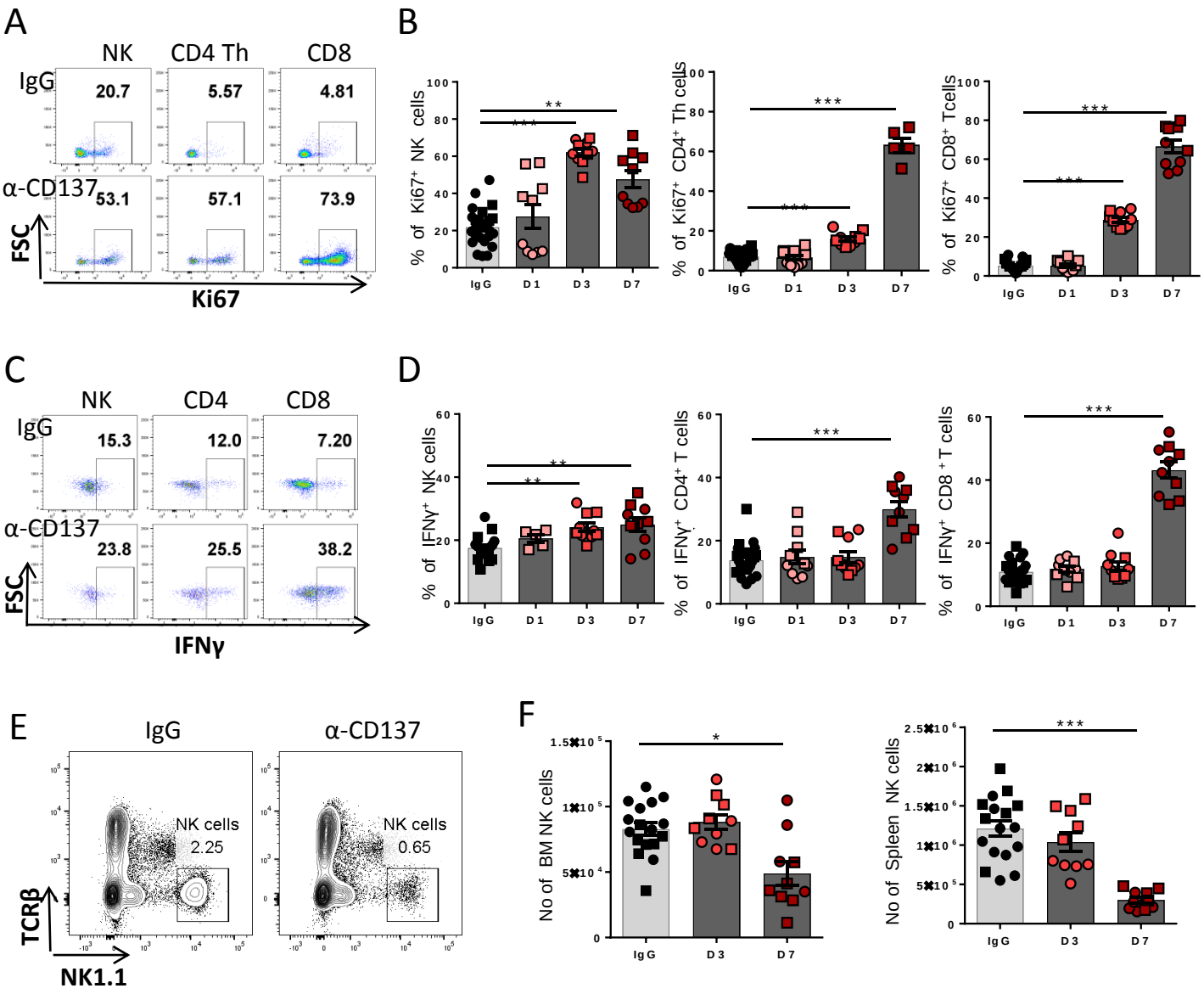

<u>Figure 3:</u> NK cells and T cells show different kinetics of response to CD137 stimulation.
Naïve WT mice received a single ip injection of 100 µg of anti-CD137 mAbs or control IgG on day 0 and analysis was performed on day 1, 3 and 7. (A, B) Proliferation of BM NK cells (NK), FoxP3$^-$ CD4$^+$ T cells (CD4 Th) and CD8$^+$ T cells (CD8) was assessed by Ki67 staining. (C, D) Total BM cells were cultured with PMA-ionomycin for 2 hrs and IFN-γ production by NK cells, CD4$^+$ T cells (CD4) and CD8$^+$ T cells was assessed by intracellular staining. (E, F) NK cell numbers in the spleen and BM were quantified by flow cytometry. Data are shown as (A, C, E) representative staining on day 7 or (B, D, F) mean ± SEM of data from 2 pooled experiments, each with n=5 mice per group. Dot-plots in E are from the spleen. Data were analyzed with a Kruskal-Wallis test followed by a Dunn's multiple comparisons post-hoc test. * $p < 0.05$; ** $p < 0.01$; *** $p < 0.001$.

Figure 4

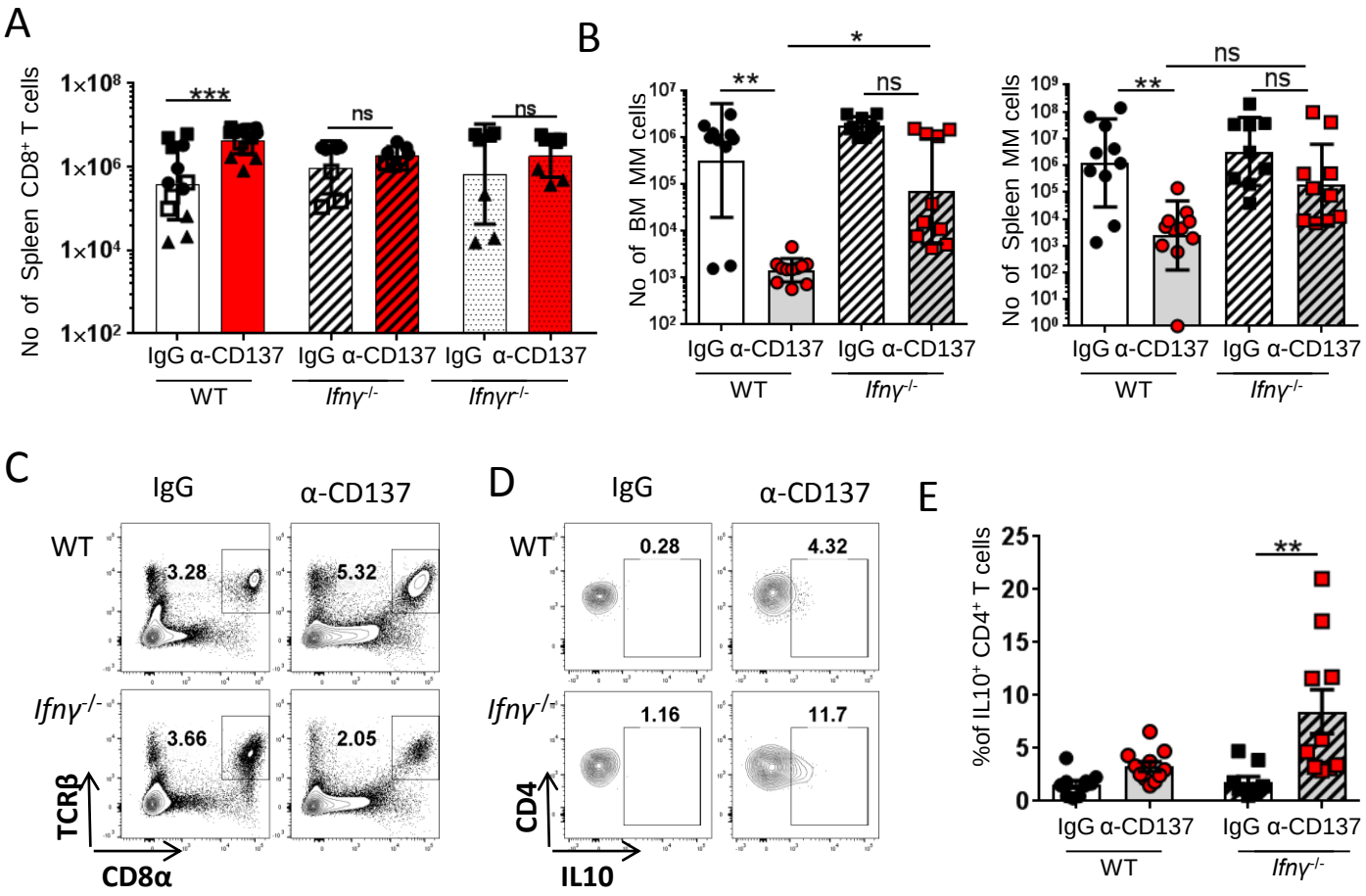

Figure 4: IFNγ signaling is required for optimal efficacy of anti-CD137 mAb therapy

(A) Naïve WT, *Ifnγ*$^{-/-}$ or *Ifnγr*$^{-/-}$ mice received a 2-week anti-CD137 mAb treatment and CD8^{+} T cell numbers in the spleen were determined by flow cytometry. The geometric means ± SD of 4 pooled experiments are shown. Data acquired within the same experiment are depicted with similar symbols. (B-E) WT or *Ifnγ*$^{-/-}$ were challenged with Vk*MYC cells and 2 weeks later, mice received a 2-week anti-CD137 mAb treatment. At week 5 post Vk*MYC cell challenge, numbers of BM (B left) or spleen (B right) MM cells as well as (C) percentages of CD8^{+} T cells within BM lymphocytes were analyzed by flow cytometry. (D-E) Total BM cells were cultured with PMA-ionomycin for 2 hrs and IL10 production by CD4^{+} T cells was determined by intracellular staining. Graphs show (B) geometric mean ± SD or (E) mean ± SEM of 1 experiment with n = 9-11 mice per group. Data were analyzed with (A) a Mann-Whitney U test or (B, E) a Kruskal-Wallis test followed by a Dunn's multiple comparison post hoc test. * $p < 0.05$; ** $p < 0.01$, *** $p < 0.001$, ns: non significant.

Figure 5

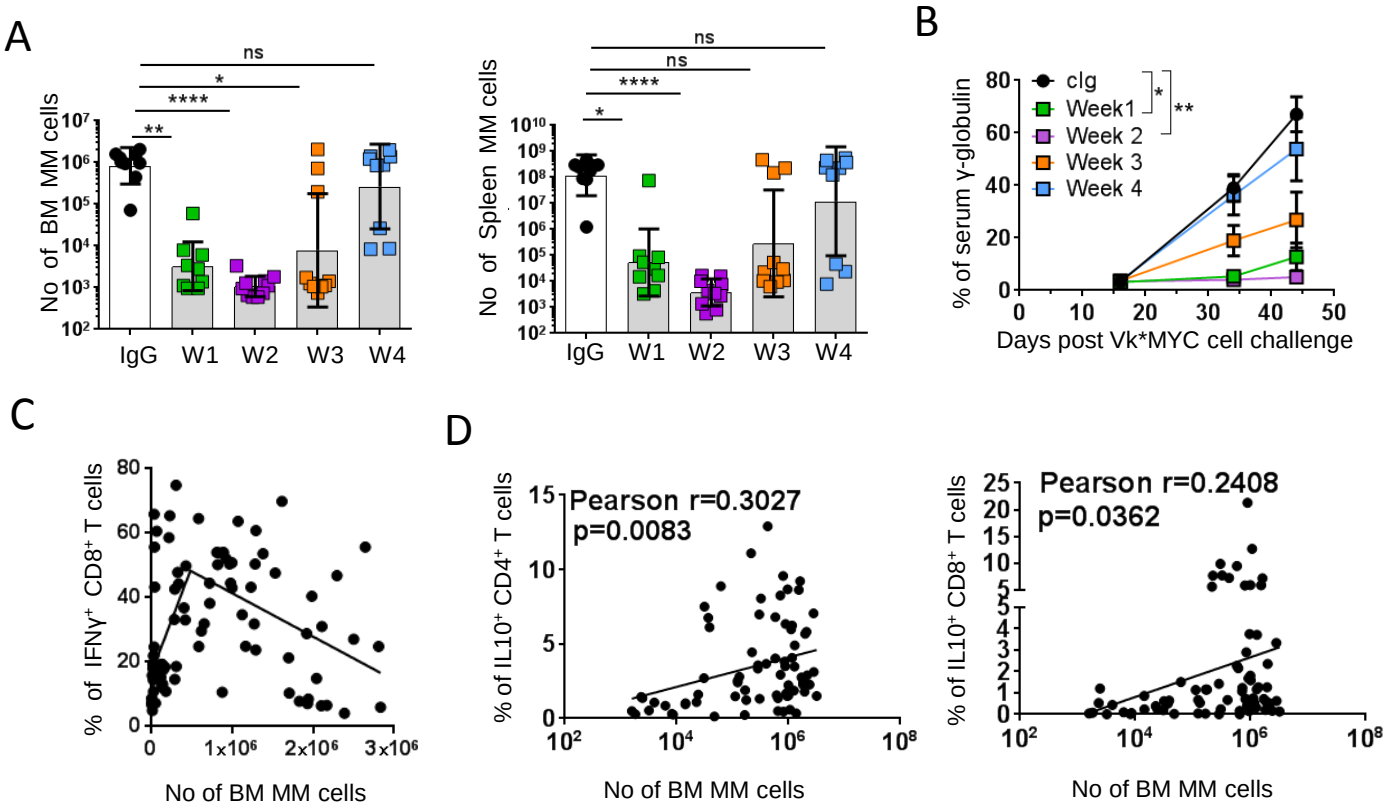

<u>Figure 5</u>: MM growth is associated with progressive immunosuppression and loss of anti-CD137 mAb treatment efficacy.

(A-B) WT mice were challenged with Vk*MYC cells and mice received a 2-week anti-CD137 mAb treatment starting from week 1, 2, 3 or 4 post Vk*MYC cell challenge (see Supplemental Figure 5C). (A) Tumor burden in the BM (left) or the spleen (right) was analyzed by flow cytometry at week 6 post Vk*MYC cell challenge. (B) Monoclonal gammopathy was analyzed over time by serum electrophoresis. Graphs display (A) the geometric mean ± SD or (B) mean ± SEM of 1 experiment with n = 9-10 mice per group. Data were analyzed with a Kruskal-Wallis test followed by a Dunn's multiple comparisons post-hoc test performed on week 6 values. * $p < 0.05$; ** $p < 0.01$; **** $p < 0.0001$, ns: non significant. (C-D) WT mice were challenged with Vk*MYC cells and 3 to 6 weeks later, BM cells were collected and cultured with PMA-ionomycin for 2 hrs. (C) IFNγ-production by $CD8^+$ T cells or (D) IL10-production by $CD4^+$ and $CD8^+$ T cells were measured by intracellular staining. Data are pooled from n=9-10 independent experiments with a total of n=76-91 mice that have either been left untreated or received control treatment (PBS or IgG). (C) Data were analyzed with the GraphPad Prism software using unconstrained segmental linear regression, $p < 0.0001$; X0 = 479425. (D) Data were analyzed with a Pearson correlation test.

Figure 6

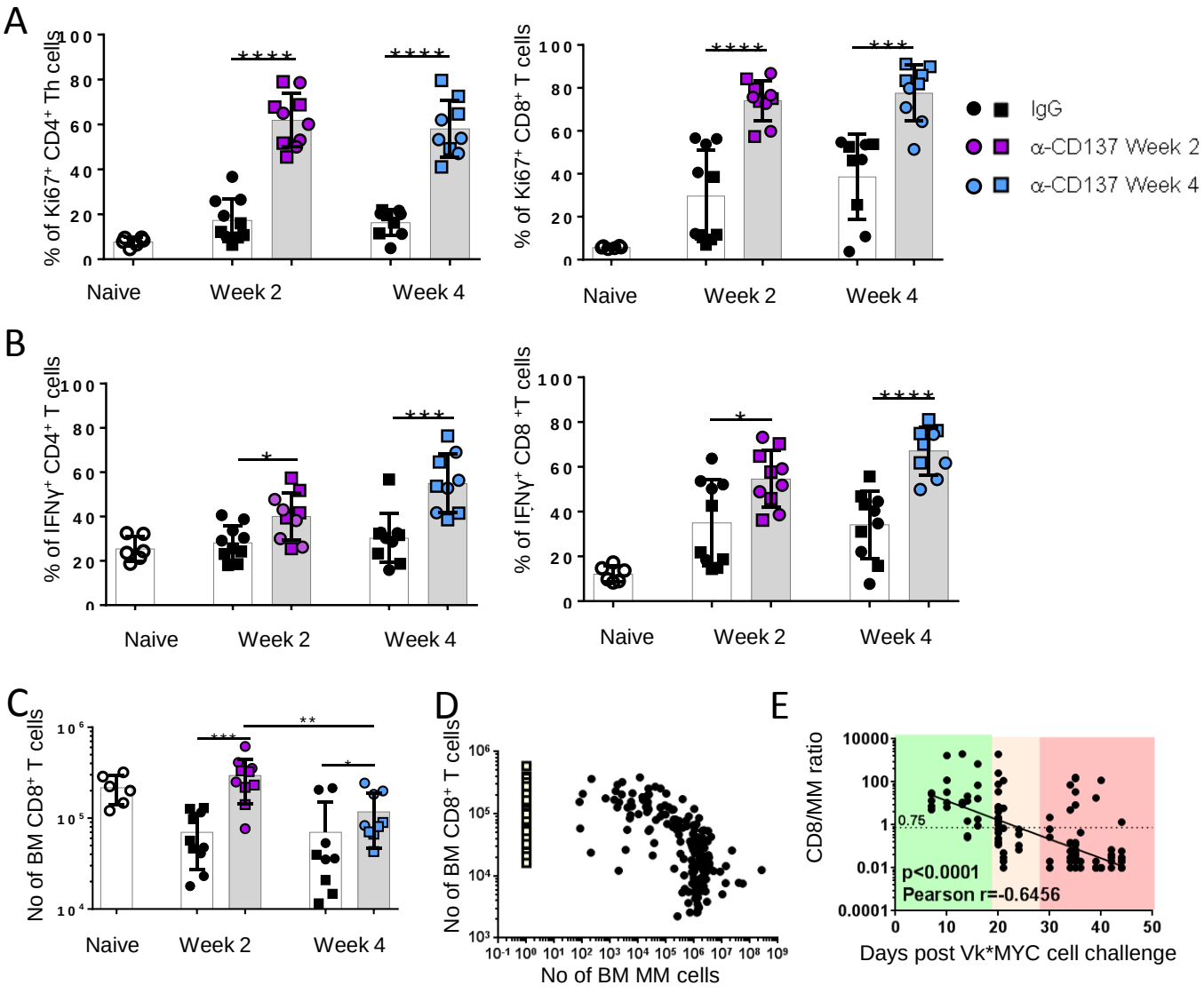

Figure 6: In mice with high MM burden, T cells are responsive to CD137 stimulation but delayed anti-CD137 mAb treatment fails to expand large numbers of CD8⁺ T cells. (A-C) WT mice received a single injection of anti-CD137 mAbs at week 2 or 4 post Vk*MYC cell challenge. T cell responses in the BM were analyzed 1 week later. Naïve mice were included as control. (A) Proliferation of $CD4^+$ Th ($FoxP3^-$) and $CD8^+$ T cells was assessed by intracellular Ki67 staining. (B) IFNγ-production by $CD4^+$ and $CD8^+$ T cells was assessed by intracellular staining. (C) $CD8^+$ T cell numbers in the BM were determined by flow cytometry. (D-E) WT mice were challenged with Vk*MYC cells (close circles) and 1 to 6 weeks later, numbers of CD8 T cell and $CD155^+$ PCs in the BM were analyzed by flow-cytometry. (D) $CD8^+$ T cells in the BM of naïve mice were analyzed as control (open squares) and have been attributed the value of 1 MM cell to be plotted on the log axis. (E) The ratio between $CD8^+$ T cells and tumor cells (CD8/MM ratio) was determined by flow cytometry at different time points. The color rectangles highlight data at time points when anti-CD137 mAb treatment generally decreases tumor growth in most of the mice (green), decreases tumor growth in only some mice (orange) or has no effect on tumor growth in most of the mice (red). Data are pooled from (A-C) n=2 independent experiments, each with n=3-5 mice per group, (D-E) n=16 independent experiments with n=60 naïve and n=171 MM-bearing mice. Data were analyzed with (A-C) a Mann-Whitney U test or (E) a Pearson correlation test, * $p < 0.05$; *** $p < 0.001$; **** $p < 0.0001$.

Figure 7

A

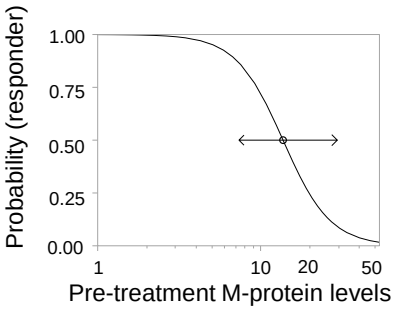

	Non-responder	Responder
Identified as non-responder	**8**	*2*
Identified as responder	*2*	**15**
Total	10	17

B

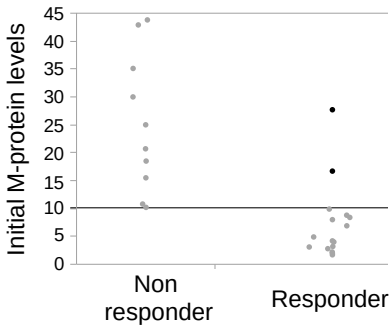

<u>Figure 7</u>: Initial MM burden determines treatment efficacy

(A-B) WT mice were challenged with Vk*MYC cells and 2-4 weeks later, serum M-protein levels were measured before the mice were given a 2 week anti-CD137 mAb treatment. Mice were categorized as responders if their serum M-protein levels after treatment were below 30 %. Data from 3 independent experiments with a total of n= 30 mice was analyzed. (A) Logistic fit (left) and corresponding confusion matrix (right) of the probability to be a non-responder versus pre-treatment M-protein levels (likelihood ratio $\chi_1^2 = 19.0$, P<0.0001). According to this analysis, mice with pre-treatment M-protein levels of 13.61 % (95% CI 7.34, 29.37) have a 50 % chance to respond to the treatment. (B) Partition tree classifying mice with pre-treatment M-protein levels < 10.2 % as responders and others as non responders.

Figure 8

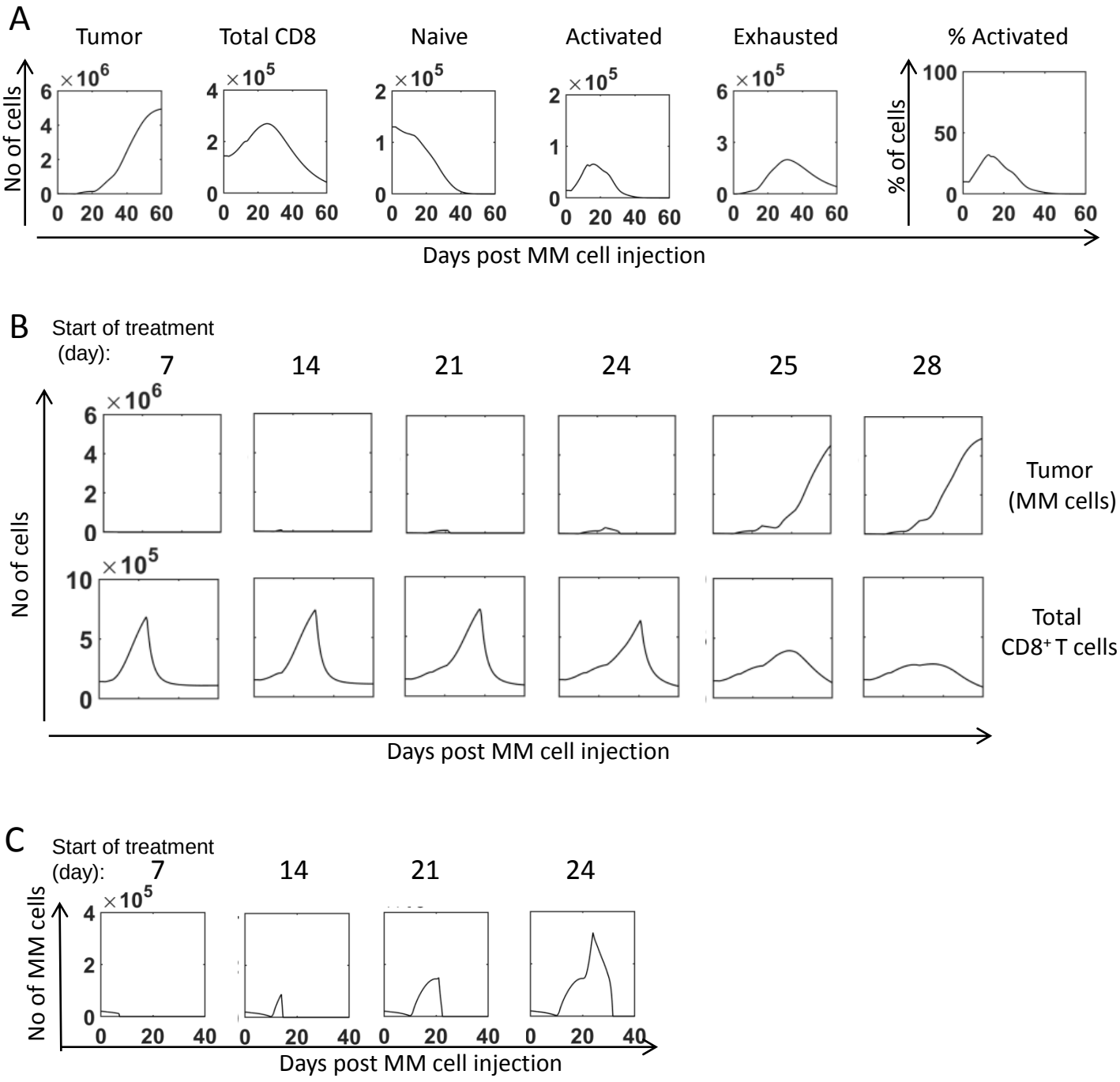

<u>Figure 8</u>: Modeling interactions between CD8⁺ T cells and MM cells in the context of anti-CD137 mAb treatment.

Dynamic interactions between MM cells and CD8⁺ T cells were modeled *in silico.* (A) Numbers of MM cells and naïve, activated and exhausted CD8⁺ T cells overtime using optimized parameters to fit the experimental data in untreated mice. (B-C) Effect of a 2-week anti-CD137 mAb started at different time points between day 7 and 28 post MM injection. (B) Graphs within a column represent the numbers of MM cells and total CD8 T cells overtime when treatment was started on a given day post MM injection (indicated at the top of each column). (C) Scale from graphs in B was adjusted to visualize the evolution of MM cell numbers when treatment was efficient.

Figure 9

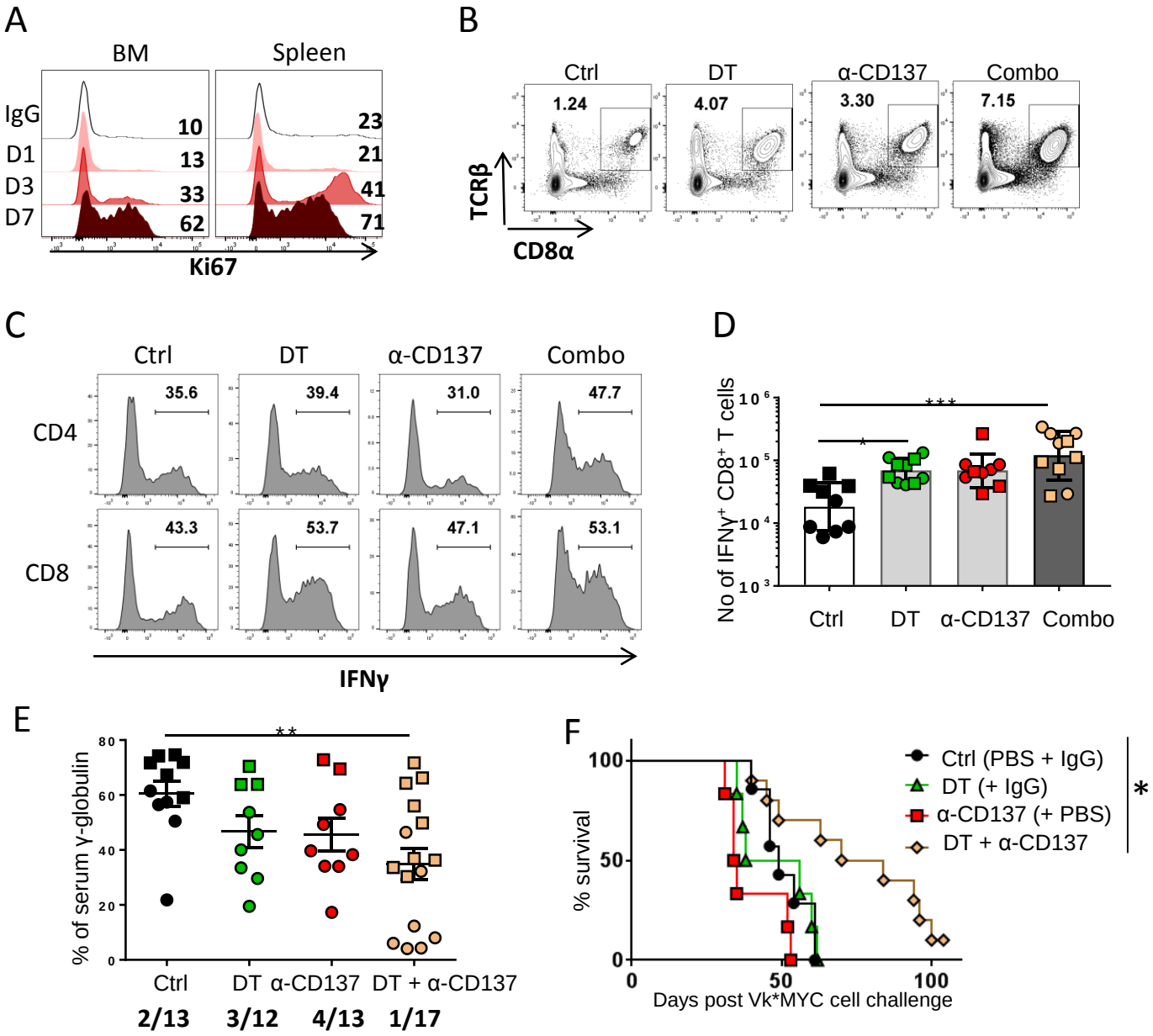

Figure 9: Treg-depletion promotes the expansion of IFNγ-producing CD8⁺ T cells in the BM and restores the efficacy of delayed anti-CD137 mAb treatment. (A) WT mice received a single anti-CD137 mAb injection on day 0 and FoxP3⁺ Treg proliferation was analyzed on day 1, 3 and 7. (B-D) FoxP3-DTR mice were challenged with Vk*MYC cells on day 0 and were given 250 ng of DT (or PBS as control) on day 21, and a single injection of anti-CD137 mAbs (or control IgG) on day 22. BM T cells were analyzed by flow cytometry on day 28. (B) CD8⁺ T cell percentages, gated on live CD45.2⁺ lymphocytes. (C) Percentages of IFNγ⁺ CD4⁺ and CD8⁺ T cells. (D) Quantification of IFNγ⁺ CD8⁺ T cell numbers. (E-F) FoxP3-DTR mice were challenged with Vk*MYC cells on day 0. Mice received 250 ng of DT on day 24 and 29, together with a 2-week anti-CD137 mAb treatment from day 25. (E) At the end of the treatment, serum M-protein levels were determined by electrophoresis. Numbers indicate the number of mice excluded (that had already succumbed to MM) over the total number of mice per group. (F) Survival was followed overtime. Data are (A-C) representative or shown as (D) geometric mean ± SD or (E) mean ± SEM of 2 experiments, each with n=5-10 mice per group. Symbol shapes identify data from independent experiments. (F) Data are from 1 experiment with n = 6-10 mice per group. Data were analyzed using (D-E) a Kruskal-Wallis test followed by a Dunn's multiple comparison post-hoc test or (H) a Log-rank test, *p < 0.05; ** p < 0. 01; *** p < 0. 001; **** p < 0.0001.

Figure 10

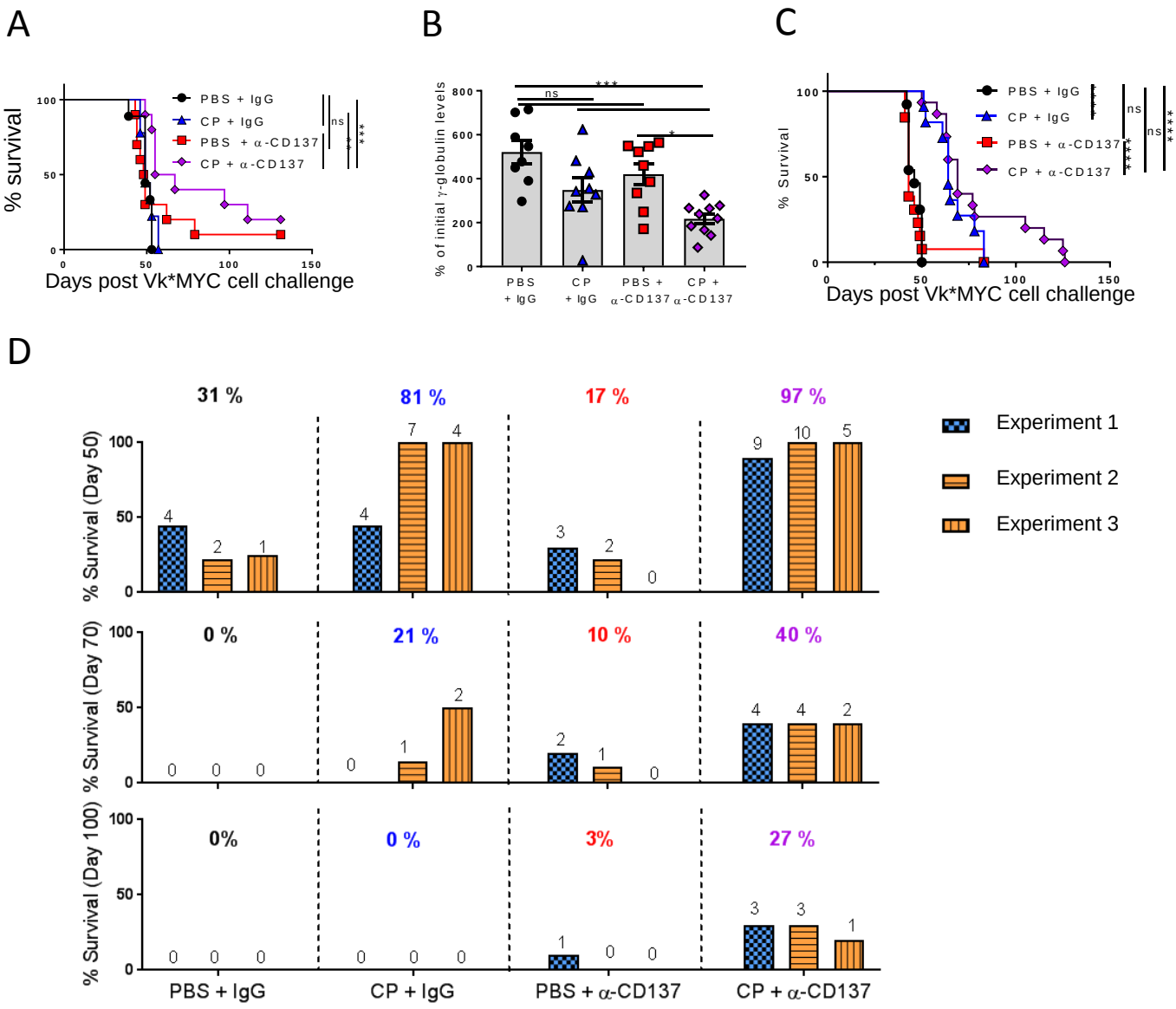

Figure 10: Anti-CD137 mAb treatment prevents relapse after cyclophosphamide treatment and allows long-term survival. C57BL/6 WT mice were challenged with Vk*MYC cells on day 0. Four weeks later, mice received a treatment consisting of 2 injections of cyclophosphamide (CP) followed by 2-week anti-CD137 mAb treatment (as explained in Supplemental Figure 10C). (A, B) Mice were injected with 25 mg/kg of CP on day 27 and 28. (A) Survival was monitored overtime. (B) Serum electrophoresis was performed on day 26 (before treatment) and on day 41 (2 weeks after the treatment started). Variation in γ-globulin levels between these 2 time points is displayed as mean ± SEM. Data are from one experiment with n=8-10 mice per group. (C) Mice were injected with 100 mg/kg of CP on day 28 and 29. Data are combined from 2 independent experiments with n=11-15 mice per group (D) Data from panel A (Experiment 1) and panel C (Experiments 2 and 3) are shown as percentages of mice alive on day 50, 70 and 100. Numbers at the top of each bar indicate the absolute number of mice alive at a given time point. The mean percentages of surviving mice within each group are indicated. Data were analyzed with a Log-rank test (A, C) or with a Kruskal-Wallis test (B). * $p < 0.05$; *** $p < 0.001$; **** $p < 0.0001$

Figure 11

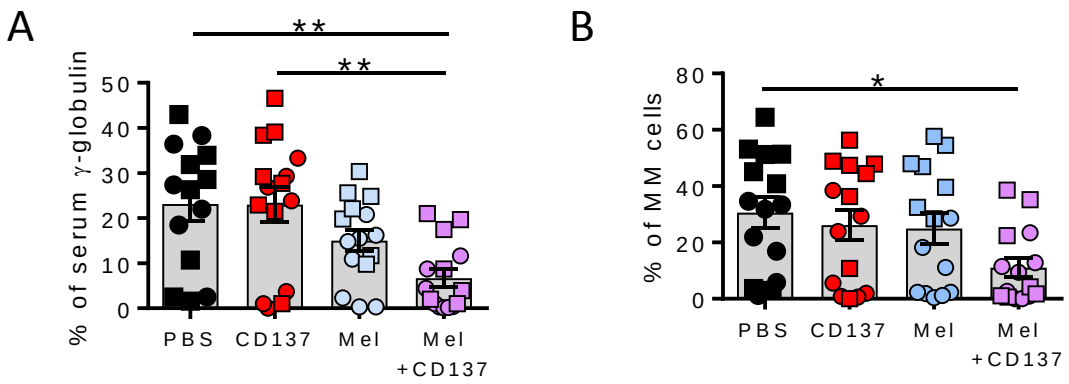

Figure 11: Sequential therapy with melphalan injections followed by anti-CD137 mAb treatment improves disease control. C57BL/6 WT mice were challenged with Vk*MYC cells on day 0. On day 21 and 22, mice were injected ip with 4mg/kg of melphalan (Mel). Mice received a 2-week anti-CD137 mAb treatment starting from day 25. On day 45, (A) serum levels of γ-globulin (M-protein) were analyzed by electrophoresis (B) percentages of MM cells in the BM were determined by flow cytometry. Data are shown as mean ± SEM of 2 experiments, each with 6-8 mice per group. Symbol shapes identify data from independent experiments. Data were analyzed with Kruskal-Wallis test followed by a Dunn's multiple comparison post-hoc test. * $p < 0.05$; ** $p < 0.01$.